

Supporting information

**Synthesis and biological evaluation of novel amino and amido substituted pentacyclic benzimidazole derivatives**

Nataša Perin<sup>1</sup>, Marjana Gulin<sup>1</sup>, Marija Kos<sup>1</sup>, Leentje Persoons<sup>2</sup>, Dirk Daelmans<sup>2</sup>, Ivana Fabijanić<sup>3</sup>, Marijana Radić Stojković<sup>3,\*</sup> and Marijana Hranjec<sup>1,\*</sup>

<sup>1</sup> Department of Organic Chemistry, Faculty of Chemical Engineering and Technology, University of Zagreb, Marulićev trg 20, HR-10000 Zagreb, Croatia;

<sup>2</sup> KU Leuven, Department of Microbiology and Immunology, Laboratory of Virology and Chemotherapy, Rega Institute, Leuven, Belgium; <sup>3</sup> Ruđer Bošković Institute, Division of Organic Chemistry and Biochemistry, Bijenička cesta 54, HR-10000 Zagreb, Croatia;

**Contents**

1. Spectroscopic characterization of pentacyclic benzimidazoles in aqueous solutions.
2. Interactions of pentacyclic benzimidazoles with ds-polynucleotides in neutral medium (pH=7.0)
  - 2.1. Fluorimetric titrations
  - 2.2. Thermal melting experiments
  - 2.3. Circular dichroism (CD) titrations
3. NMR spectra of synthesized compounds (S18-S59)

## 1. Spectroscopic characterization of pentacyclic benzimidazoles in aqueous solutions

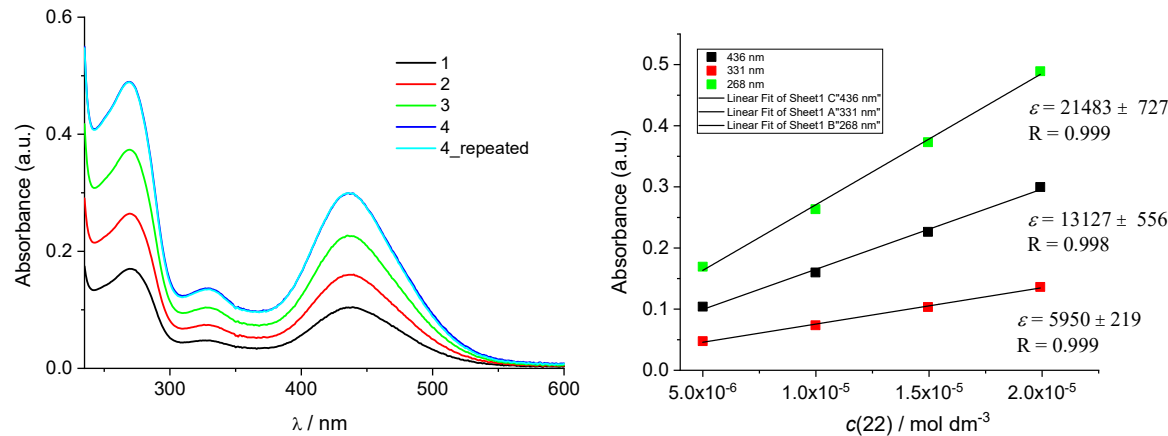


**Figure S1.** UV/Vis spectra changes of **22** at different concentrations (concentration range from  $5.0 \times 10^{-6}$  to  $2.0 \times 10^{-5}$  mol dm<sup>-3</sup>) at pH=7.0, sodium cacodylate buffer,  $I=0.05$  M.

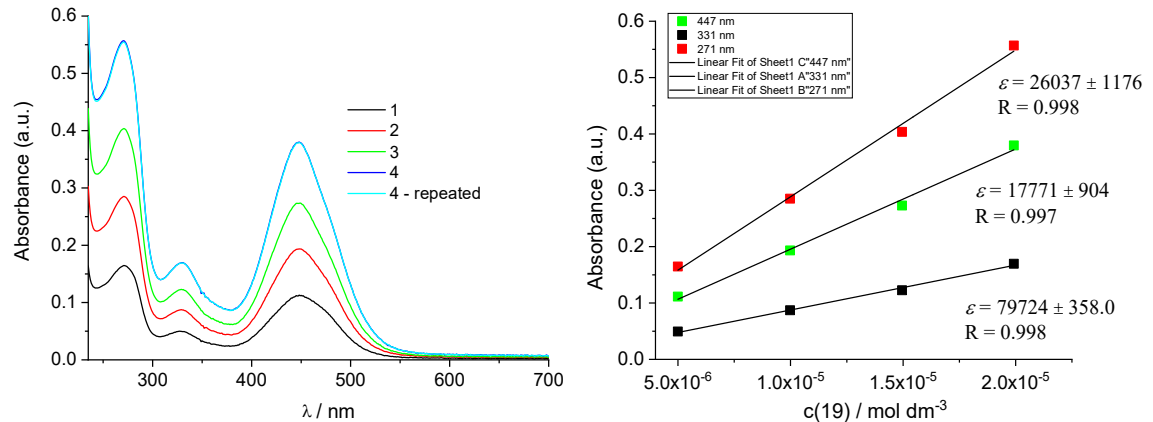


**Figure S2.** UV/Vis spectra changes of **19** at different concentrations (concentration range from  $5.0 \times 10^{-6}$  to  $1.99 \times 10^{-5}$  mol dm<sup>-3</sup>) at pH=7.0, sodium cacodylate buffer,  $I=0.05$  M.

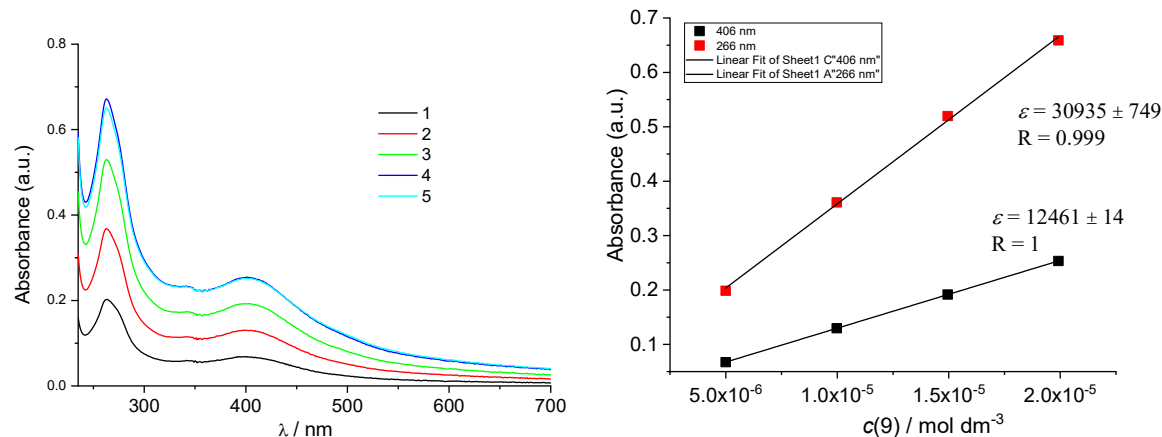


**Figure S3.** UV/Vis spectra changes of **9** at different concentrations (concentration range from  $5.0 \times 10^{-6}$  to  $1.99 \times 10^{-5}$  mol dm<sup>-3</sup>) at pH=7.0, sodium cacodylate buffer,  $I=0.05$  M.

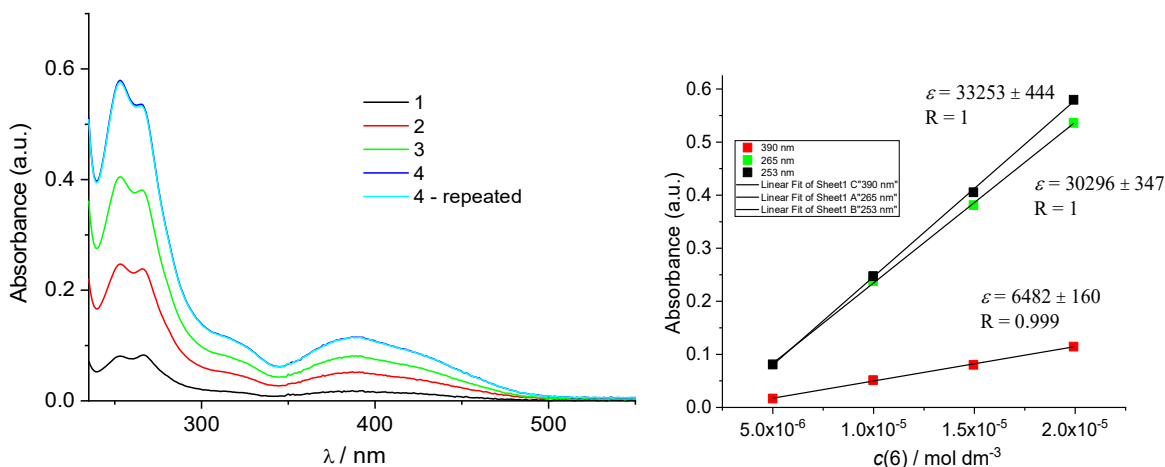


**Figure S4.** UV/Vis spectra changes of **6** at different concentrations (concentration range from  $5.0 \times 10^{-6}$  to  $1.99 \times 10^{-5}$  mol dm<sup>-3</sup>) at pH=7.0, sodium cacodylate buffer,  $I=0.05$  M.

**Table S1.** Electronic absorption data of **6**, **9**, **19** and **22**.

		pH = 7.0 <sup>a</sup>	
		$\lambda_{\text{max}}$ / nm	$\varepsilon \times 10^3$ / mmol <sup>-1</sup> cm <sup>2</sup>
<b>6</b>	253	33.25	
	265	30.30	
	390	6.48	
<b>9</b>	266	30.93	
	406	12.46	
<b>19</b>	271	26.04	
	447	17.77	
<b>22</b>	268	21.48	
	436	13.13	

<sup>a</sup> Sodium cacodylate buffer,  $I = 0.05$  mol dm<sup>-3</sup>, pH = 7.0.

The emission intensities of buffered aqueous solutions (sodium cacodylate buffer,  $I = 0.05$  mol dm<sup>-3</sup>, pH = 7.0) of studied compounds were proportional to their concentrations up to  $c = 2.0 \times 10^{-6}$  mol dm<sup>-3</sup> (Figures S5-S8).

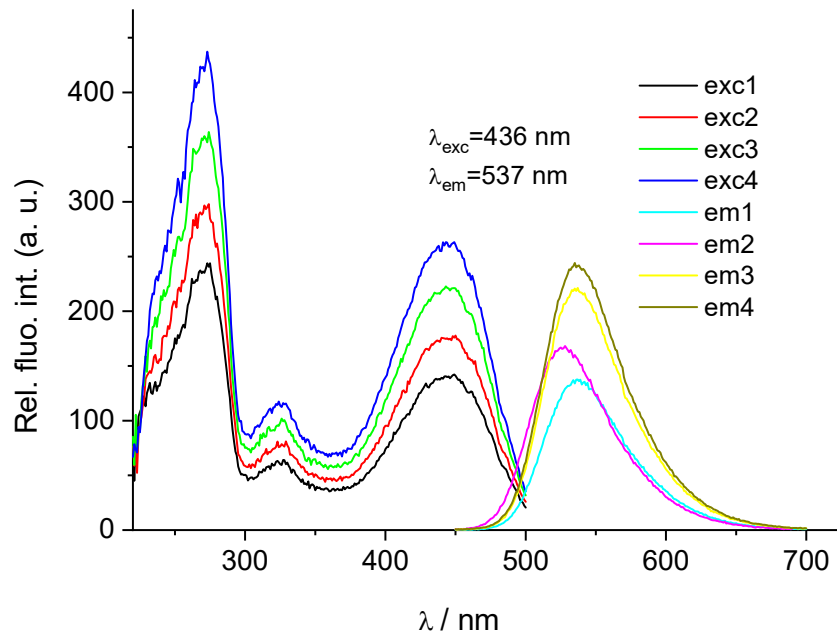


**Figure S5.** Emission and excitation spectra changes of **22** at different concentrations at  $\lambda_{\text{exc}}=436 \text{ nm}$  (concentration range from  $5.0 \times 10^{-7}$  to  $2.0 \times 10^{-6} \text{ mol dm}^{-3}$ ) at pH=7.0, Na cacodylate buffer,  $I=0.05 \text{ mol dm}^{-3}$ .

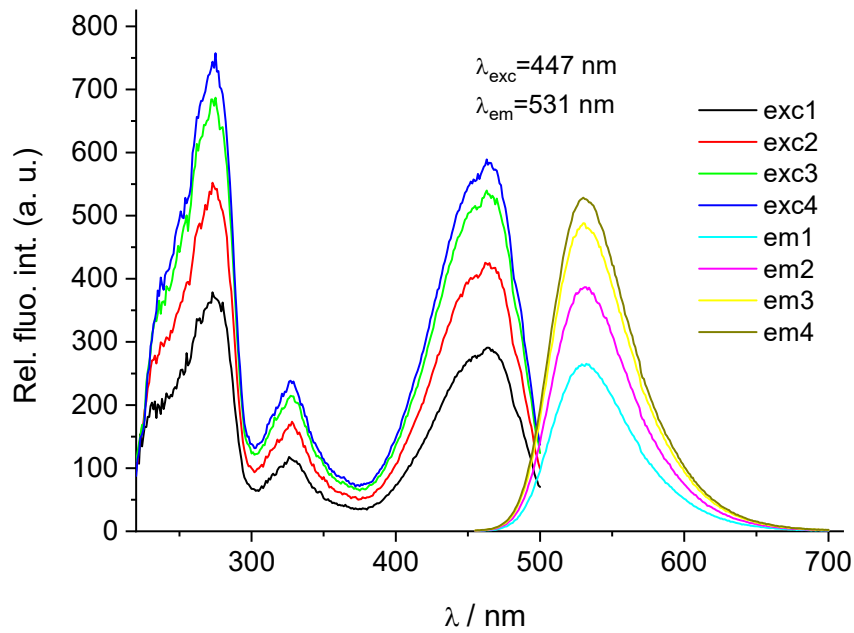


**Figure S6.** Emission and excitation spectra changes of **19** at different concentrations at  $\lambda_{\text{exc}}=447 \text{ nm}$  (concentration range from  $5.0 \times 10^{-7}$  to  $2.0 \times 10^{-6} \text{ mol dm}^{-3}$ ) at pH=7.0, Na cacodylate buffer,  $I=0.05 \text{ mol dm}^{-3}$ .

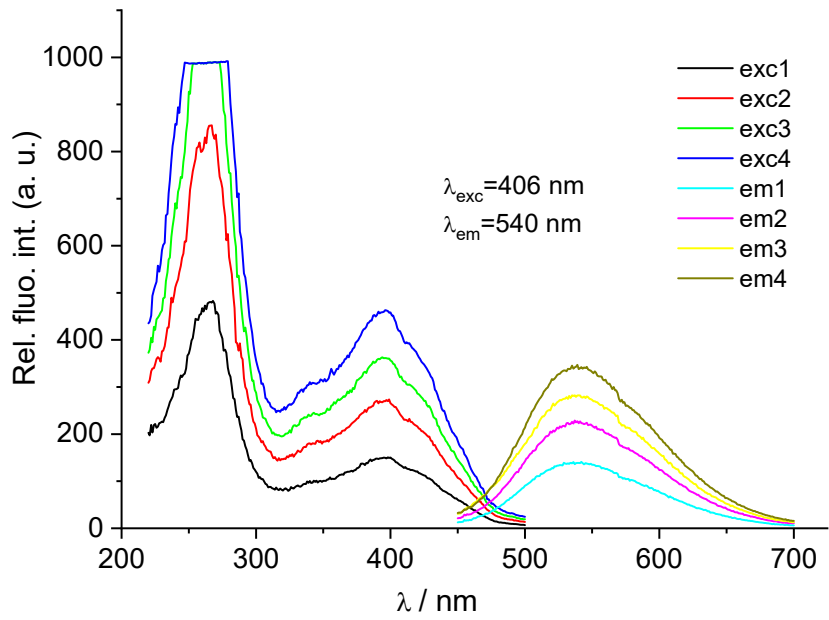


**Figure S7.** Emission and excitation spectra changes of **9** at different concentrations at  $\lambda_{\text{exc}}=406 \text{ nm}$  (concentration range from  $5.0 \times 10^{-7}$  to  $2.0 \times 10^{-6} \text{ mol dm}^{-3}$ ) at pH=7.0, Na cacodylate buffer,  $I=0.05 \text{ mol dm}^{-3}$ .

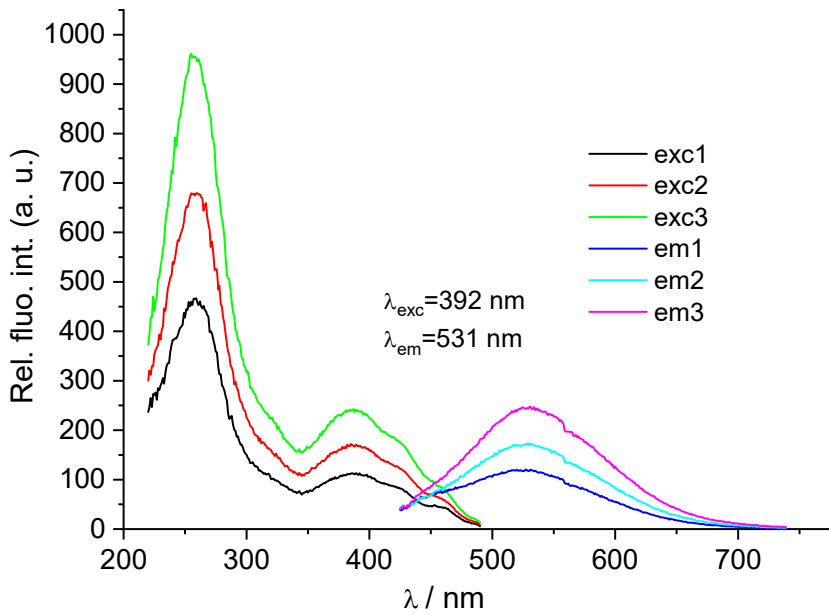


**Figure S8.** Emission and excitation spectra changes of **6** at different concentrations at  $\lambda_{\text{exc}}=392 \text{ nm}$  (concentration range from  $5.0 \times 10^{-7}$  to  $2.0 \times 10^{-6} \text{ mol dm}^{-3}$ ) at pH=7.0, Na cacodylate buffer,  $I=0.05 \text{ mol dm}^{-3}$ .

## 2. Interactions of pentacyclic benzimidazoles with ds-polynucleotides in neutral medium (pH=7.0)

### 2.1. Fluorimetric titrations

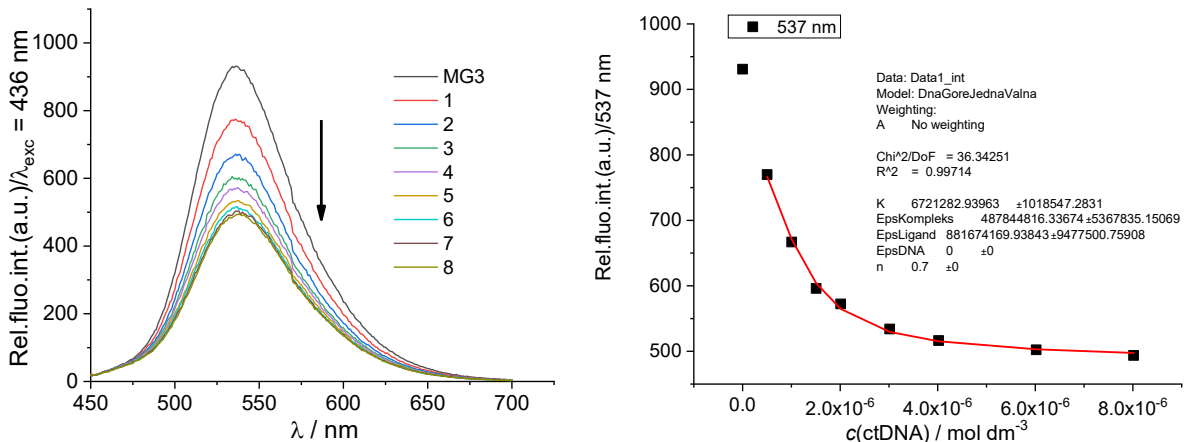


**Figure S9.** a) Changes in fluorescence spectrum of **22** ( $c = 1.0 \times 10^{-6}$  mol dm<sup>-3</sup>,  $\lambda_{\text{exc}} = 436$  nm) upon titration with ctDNA ( $c = 5.0 \times 10^{-7} - 8.0 \times 10^{-6}$  mol dm<sup>-3</sup>); b) Dependence of **22** absorbance at  $\lambda_{\text{max}} = 537$  nm on  $c(\text{ctDNA})$ , at pH=7.0, sodium cacodylate buffer,  $I = 0.05$  mol dm<sup>-3</sup>.

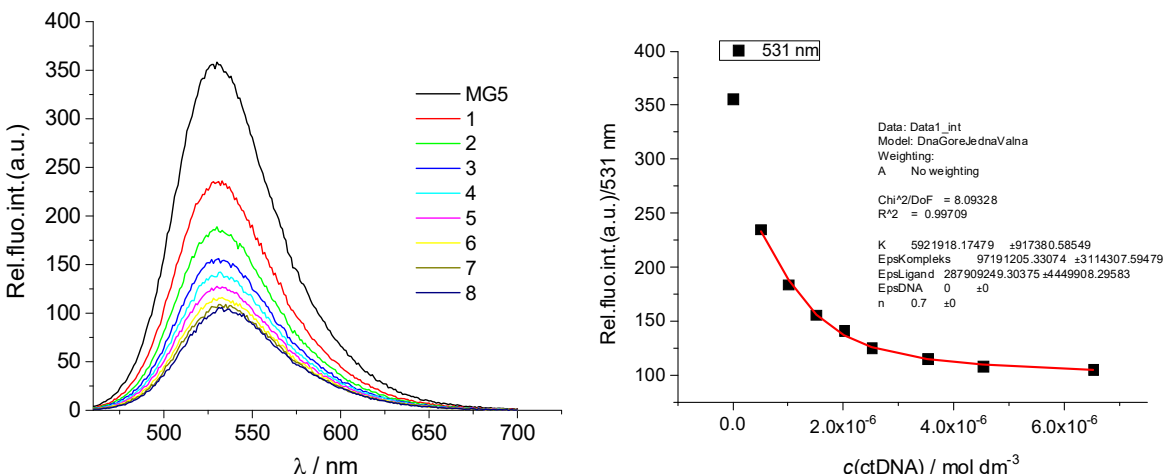


**Figure S10.** a) Changes in fluorescence spectrum of **19** ( $c = 1.0 \times 10^{-6}$  mol dm<sup>-3</sup>,  $\lambda_{\text{exc}} = 447$  nm) upon titration with ctDNA ( $c = 5.0 \times 10^{-7} - 6.5 \times 10^{-6}$  mol dm<sup>-3</sup>); b) Dependence of **19** absorbance at  $\lambda_{\text{max}} = 531$  nm on  $c(\text{ctDNA})$ , at pH=7.0, sodium cacodylate buffer,  $I = 0.05$  mol dm<sup>-3</sup>.

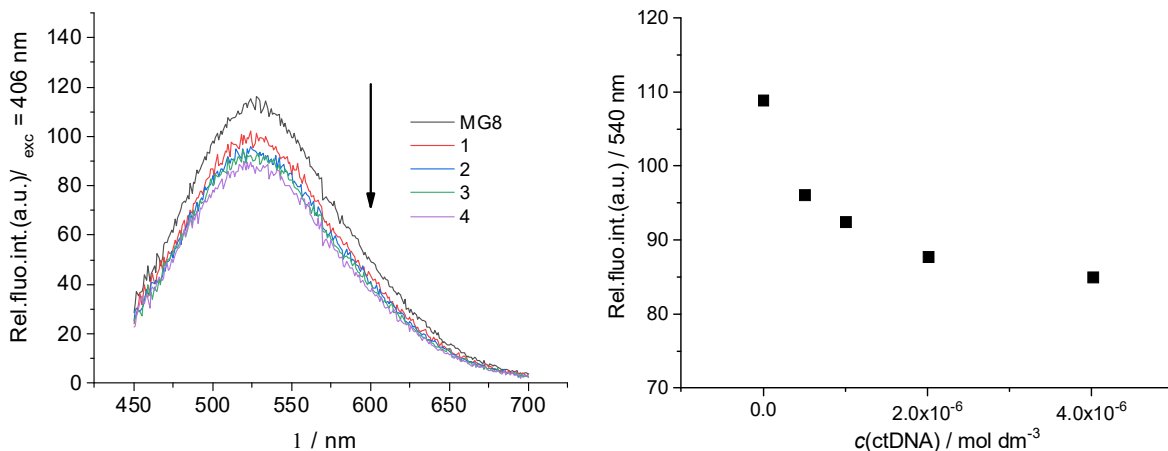


**Figure S11.** a) Changes in fluorescence spectrum of **9** ( $c = 1.0 \times 10^{-6}$  mol dm<sup>-3</sup>,  $\lambda_{\text{exc}} = 406$  nm) upon titration with ctDNA ( $c = 5.0 \times 10^{-7} - 4.0 \times 10^{-6}$  mol dm<sup>-3</sup>); b) Dependence of **9** absorbance at  $\lambda_{\text{max}} = 540$  nm on  $c(\text{ctDNA})$ , at pH=7.0, sodium cacodylate buffer,  $I = 0.05$  mol dm<sup>-3</sup>.

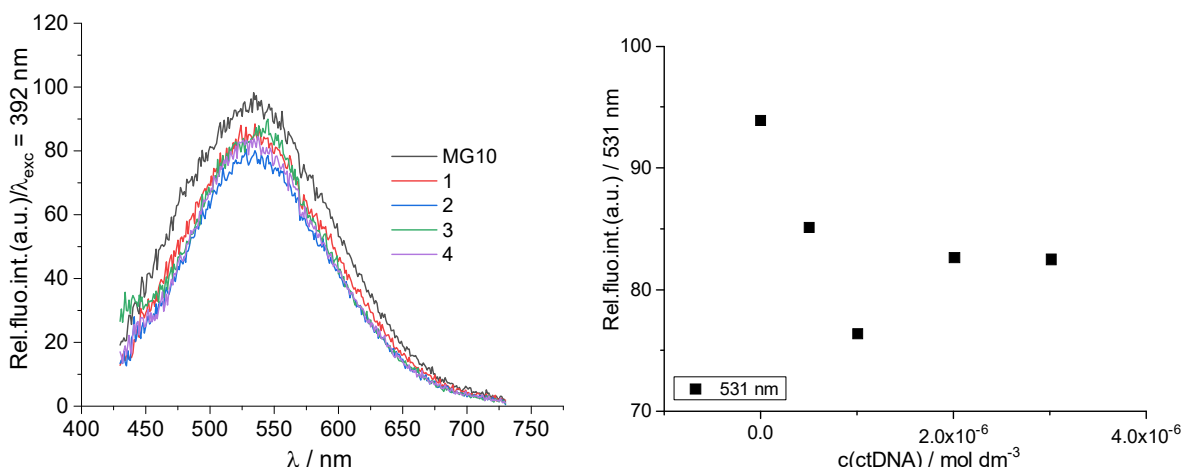


**Figure S12.** a) Changes in fluorescence spectrum of **6** ( $c = 1.0 \times 10^{-6}$  mol dm<sup>-3</sup>,  $\lambda_{\text{exc}} = 392$  nm) upon titration with ctDNA ( $c = 5.0 \times 10^{-7} - 4.0 \times 10^{-6}$  mol dm<sup>-3</sup>); b) Dependence of **6** absorbance at  $\lambda_{\text{max}} = 531$  nm on  $c(\text{ctDNA})$ , at pH=7.0, sodium cacodylate buffer,  $I = 0.05$  mol dm<sup>-3</sup>.

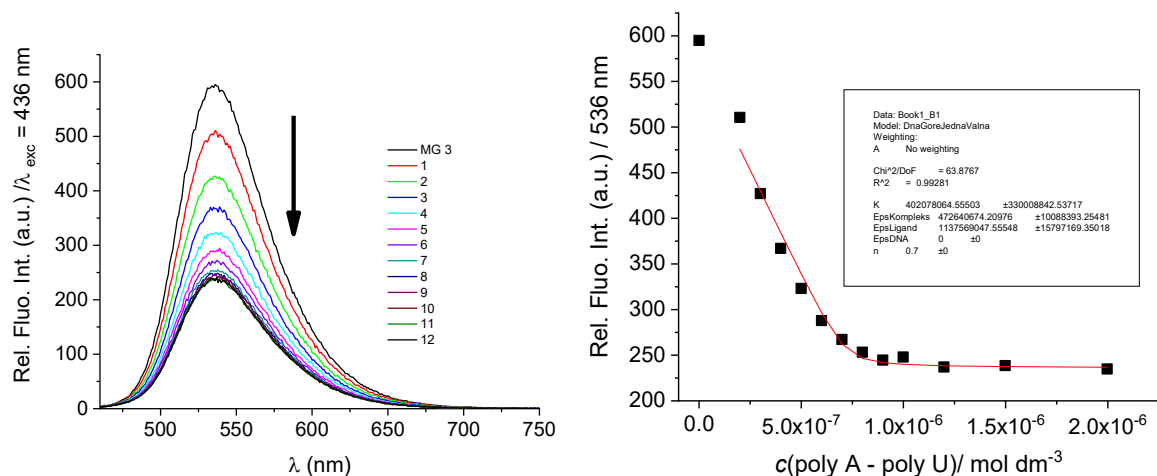


**Figure S13.** a) Changes in fluorescence spectrum of **22** ( $c = 5.0 \times 10^{-7}$  mol dm $^{-3}$ ,  $\lambda_{\text{exc}} = 436$  nm) upon titration with rArU ( $c = 2.0 \times 10^{-7} - 2.0 \times 10^{-6}$  mol dm $^{-3}$ ); b) Dependence of **22** absorbance at  $\lambda_{\text{max}} = 536$  nm on c(rArU), at pH=7.0, sodium cacodylate buffer,  $I = 0.05$  mol dm $^{-3}$ .

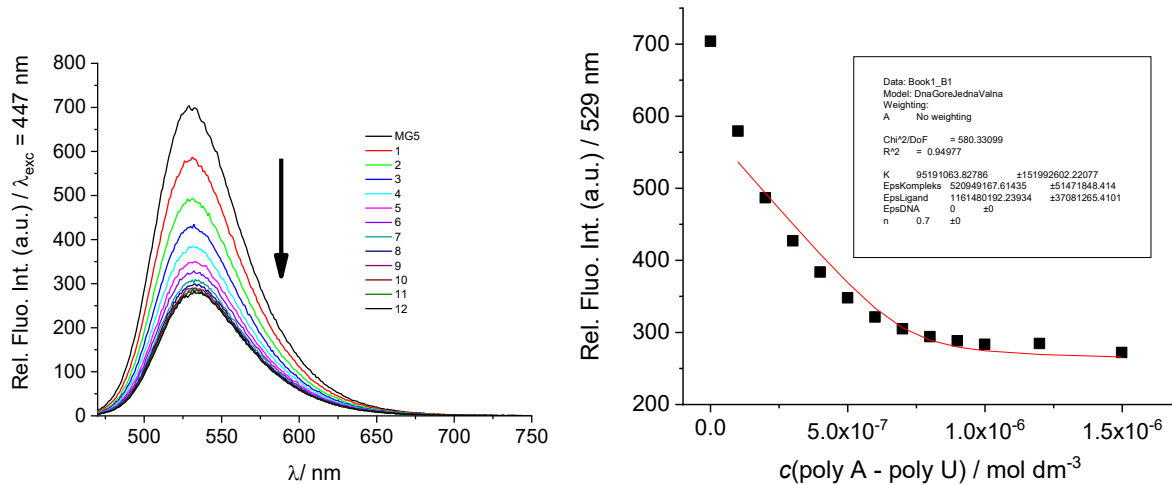


**Figure S14.** a) Changes in fluorescence spectrum of **19** ( $c = 5.0 \times 10^{-7}$  mol dm $^{-3}$ ,  $\lambda_{\text{exc}} = 447$  nm) upon titration with rArU ( $c = 1.0 \times 10^{-7} - 1.5 \times 10^{-6}$  mol dm $^{-3}$ ); b) Dependence of **19** absorbance at  $\lambda_{\text{max}} = 529$  nm on c(rArU), at pH=7.0, sodium cacodylate buffer,  $I = 0.05$  mol dm $^{-3}$ .

## 2.2. Thermal melting experiments

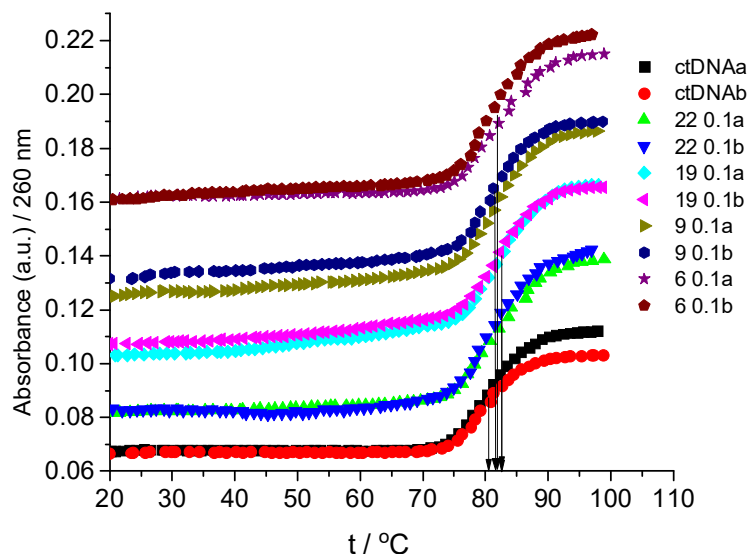


**Figure S15.** Melting curve of ctDNA upon addition of ratio,  $r$  ([compound/ [polynucleotide])] = 0.1 of **6**, **9**, **19** and **22** at pH = 7.0 (buffer sodium cacodylate,  $I = 0.05$  mol dm $^{-3}$ ).

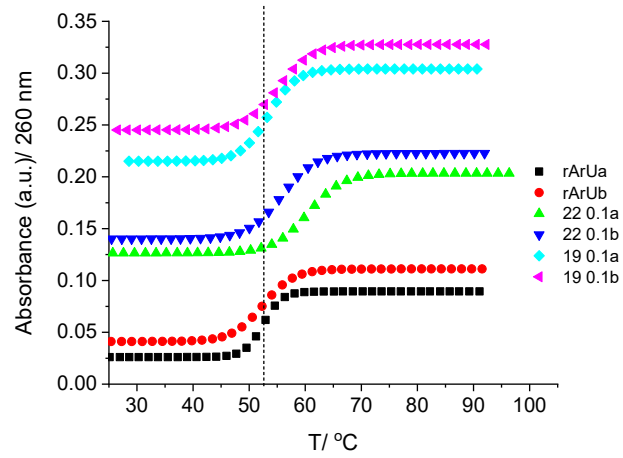


**Figure S16.** Melting curve of **rArU** upon addition of ratio, *r* ([compound/ [polynucleotide])] = 0.1 of **19** and **22** at pH = 7.0 (buffer sodium cacodylate, *I* = 0.05 mol dm<sup>-3</sup>).

### 2.3. Circular dichroism (CD) titrations

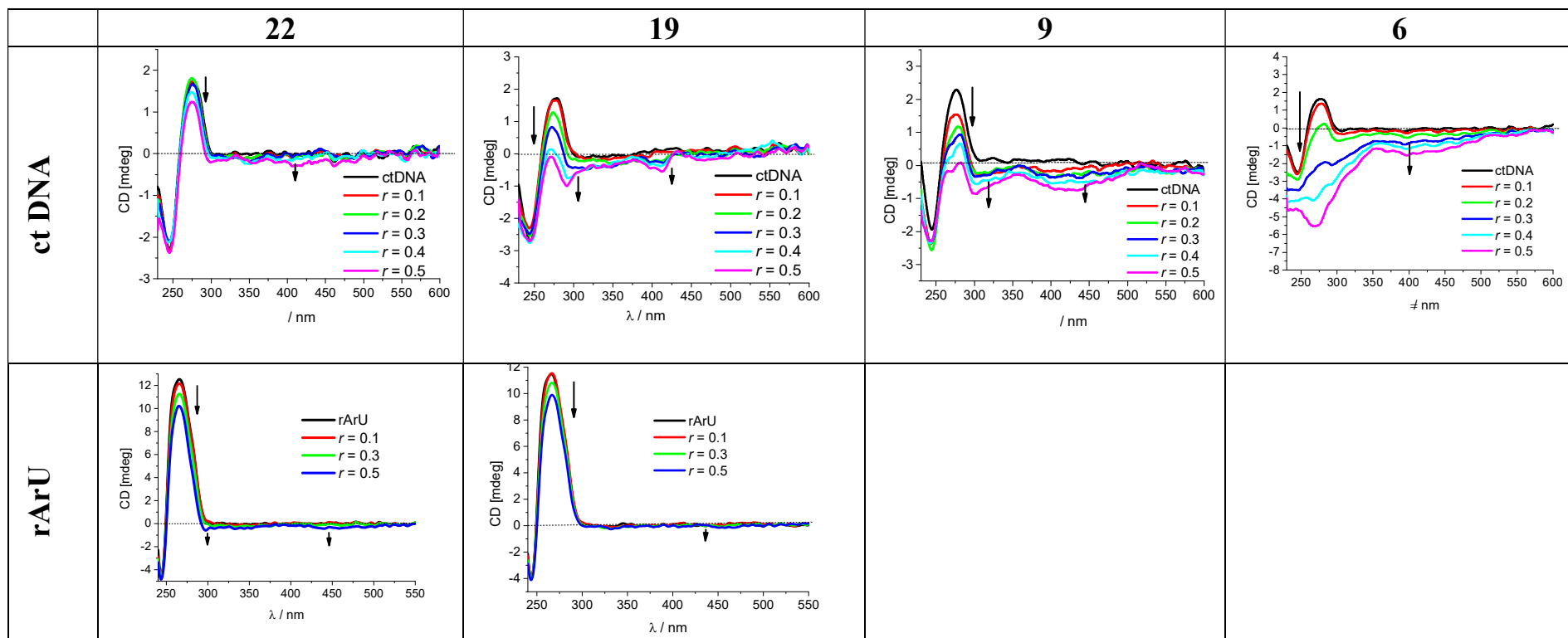


**Figure S17.** CD titration of ctDNA and rArU ( $c = 3.0 \times 10^{-5} \text{ mol dm}^{-3}$ ) with **6**, **9**, **19** and **22** at molar ratios  $r = [\text{compound}] / [\text{polynucleotide}]$  ( $\text{pH} = 7.0$ , buffer sodium cacodylate,  $I = 0.05 \text{ mol dm}^{-3}$ ).

### 3. NMR spectra of synthesized compounds

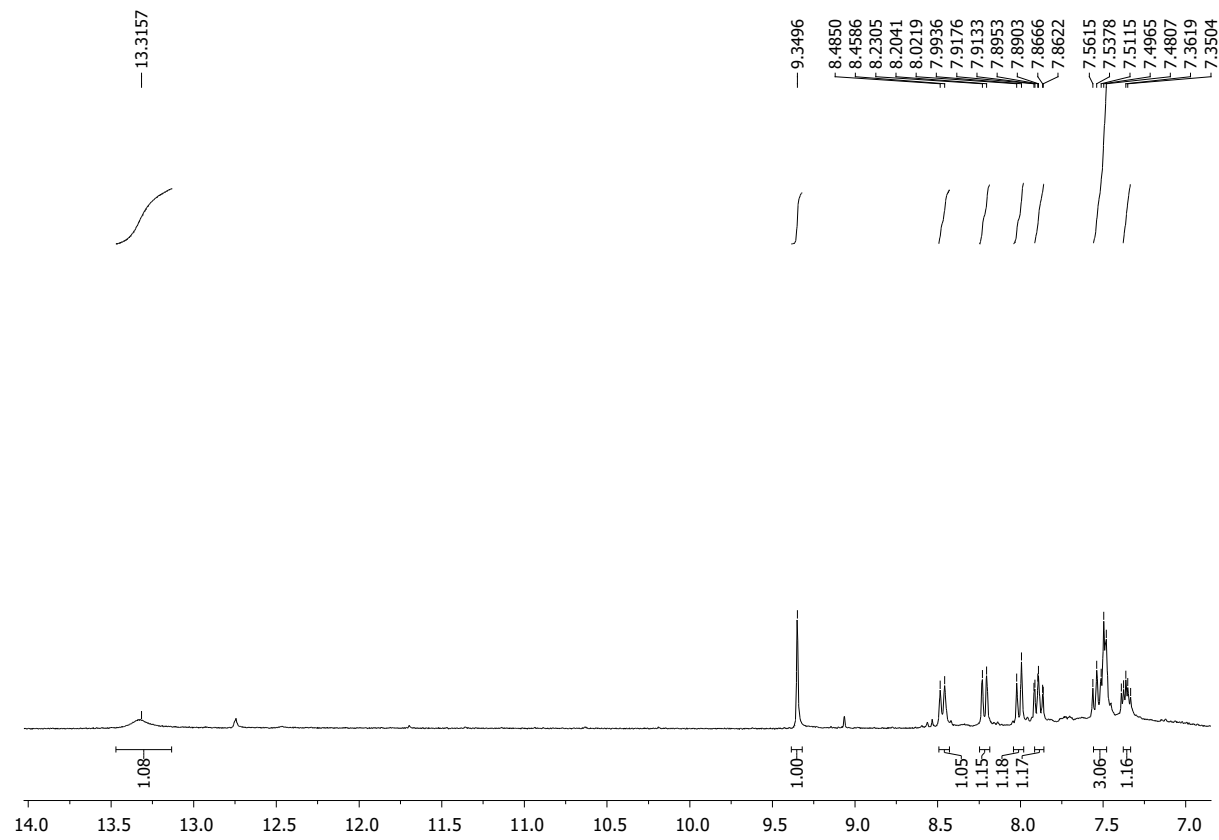


**Figure S18.** <sup>1</sup>H NMR spectrum (DMSO-*d*<sub>6</sub>, 300 MHz) of 7-oxo-5,7-dihydrobenzo[*g*]benzo[4,5]imidazo[1,2-*a*][1,8]naphthyridine-6-carbonitrile **4**

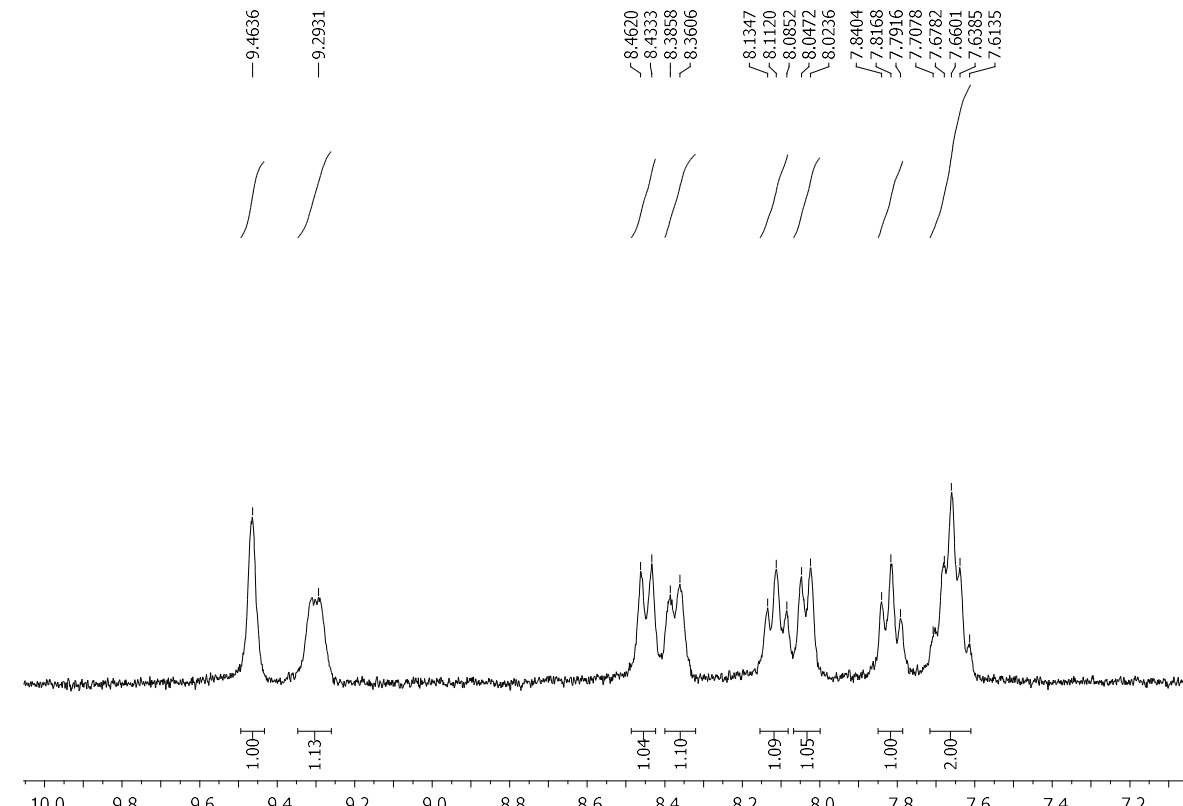


**Figure S19.** <sup>1</sup>H NMR spectrum (DMSO-*d*<sub>6</sub>, 300 MHz) of 7-chlorobenzo[*g*]benzo[4,5]imidazo[1,2-*a*][1,8]naphthyridine-6-carbonitrile **5**

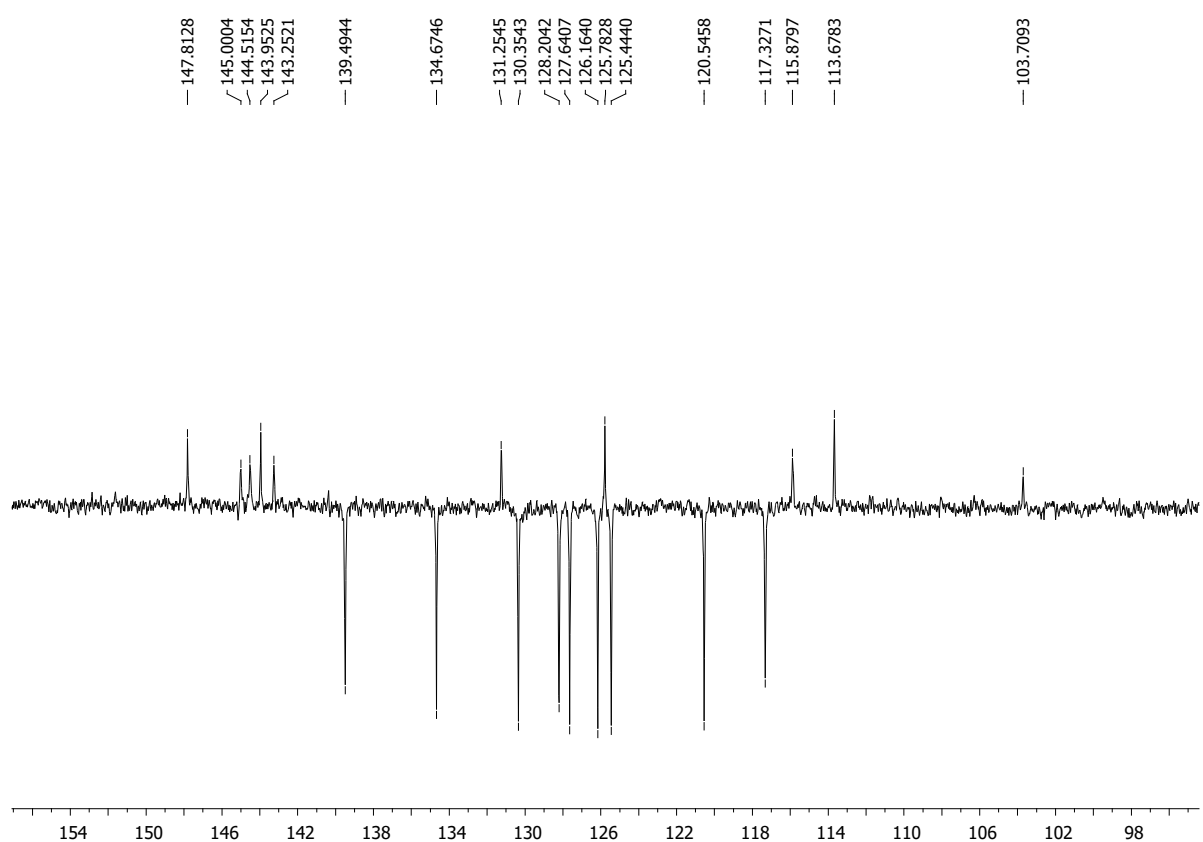


**Figure S20.** <sup>13</sup>C NMR spectrum (DMSO-d<sub>6</sub>, 100 MHz) of 7-chlorobenzo[g]benzo[4,5]imidazo[1,2-a][1,8]naphthyridine-6-carbonitrile **5**

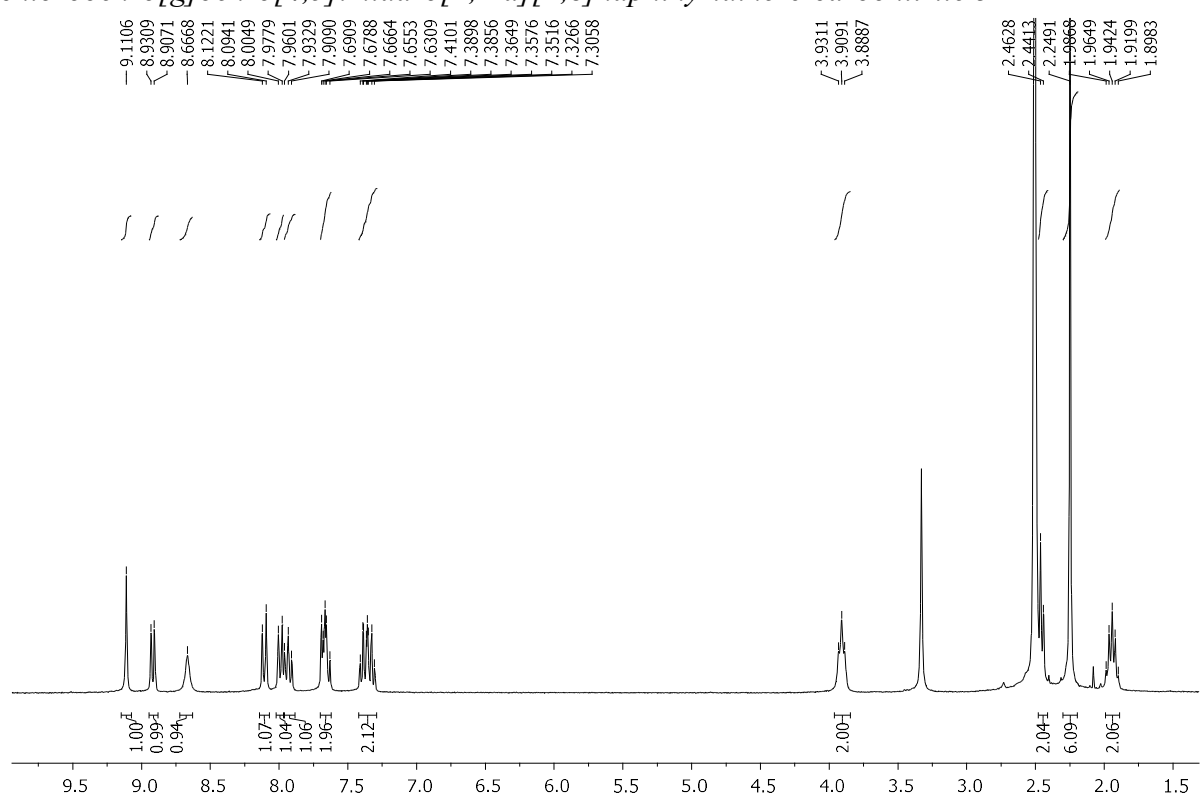


**Figure S21.** <sup>1</sup>H NMR spectrum (DMSO-d<sub>6</sub>, 300 MHz) of 7-((3-N,N-(dimethylamino)propyl)amino)benzo[g]benzo[4,5]imidazo[1,2-a][1,8]naphthyridine-6-carbonitrile **6**

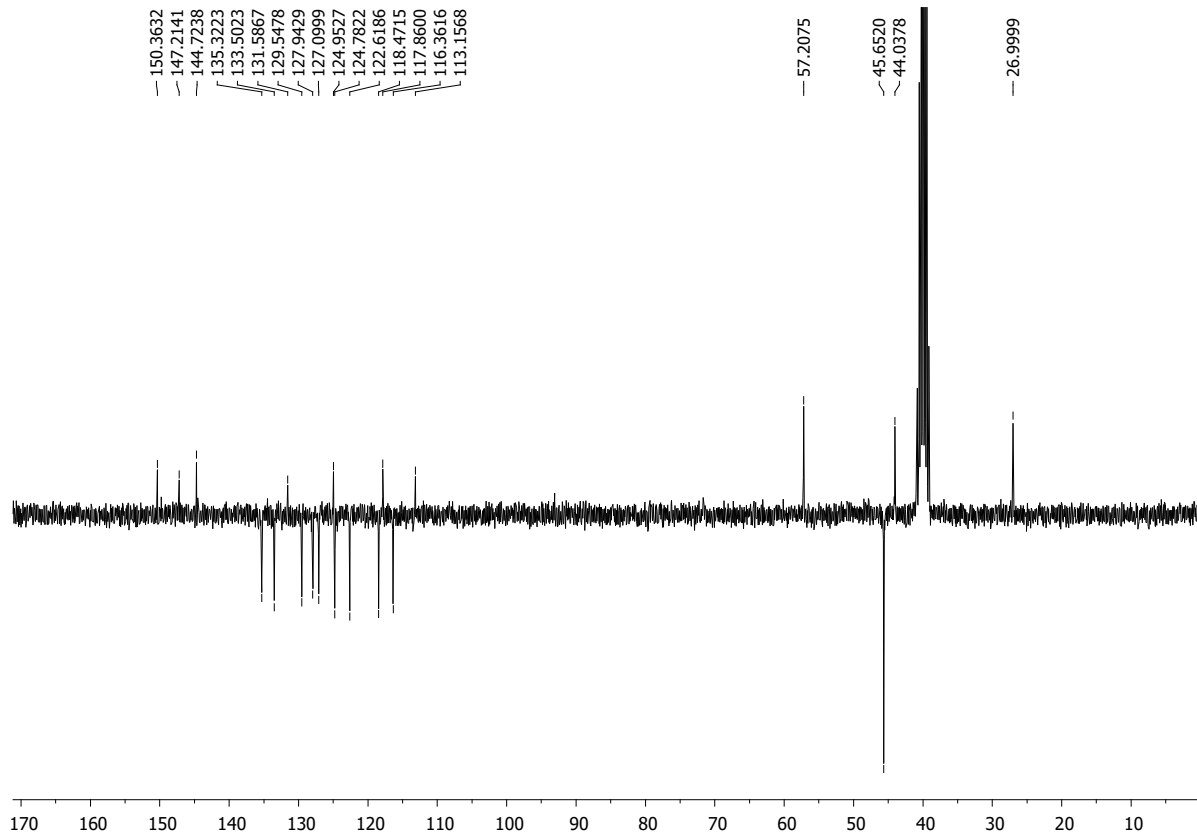


**Figure S22.**  $^{13}\text{C}$  NMR spectrum (DMSO- $d_6$ , 75 MHz) of 7-((3-*N,N*-dimethylamino)propyl)amino)benzo[*g*]benzo[4,5]imidazo[1,2-*a*][1,8]naphthyridine-6-carbonitrile **6**

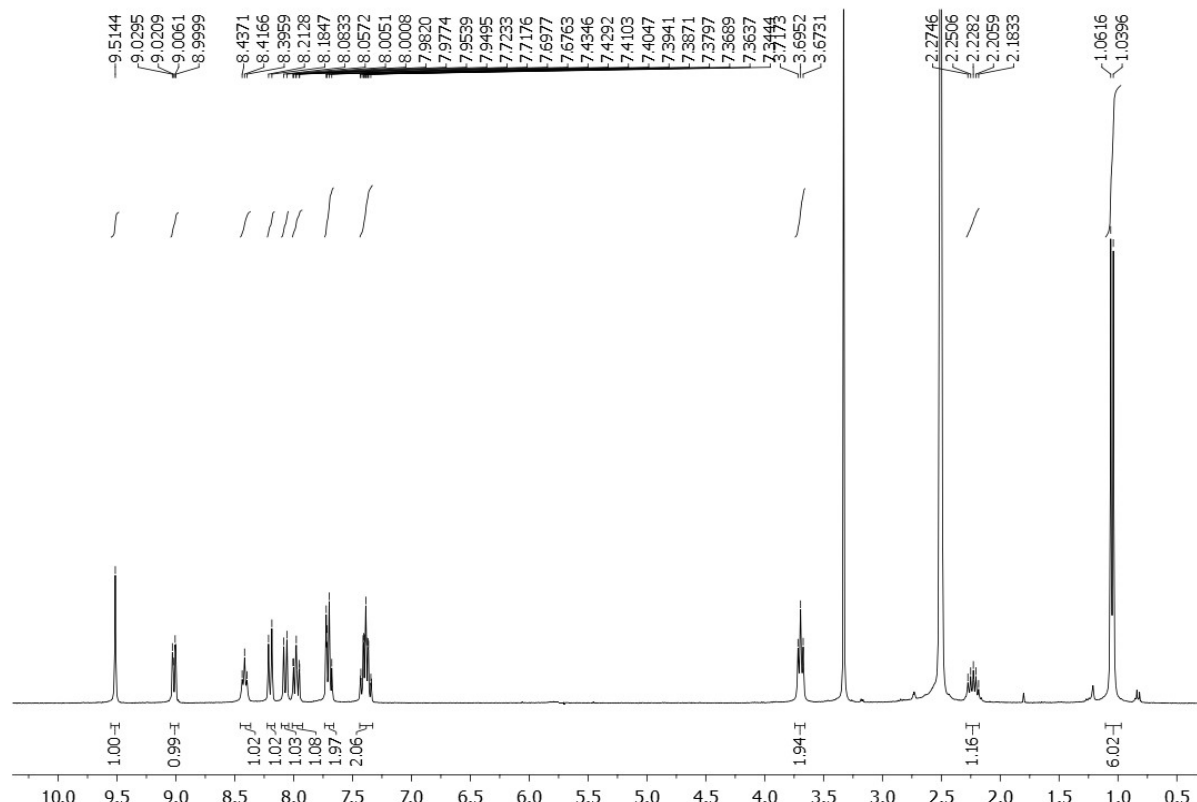


**Figure S23.**  $^1\text{H}$  NMR spectrum (DMSO- $d_6$ , 300 MHz) of 7-(*N*-isobutylamino)benzo[*g*]benzo[4,5]imidazo[1,2-*a*][1,8]naphthyridine-6-carbonitrile **7**

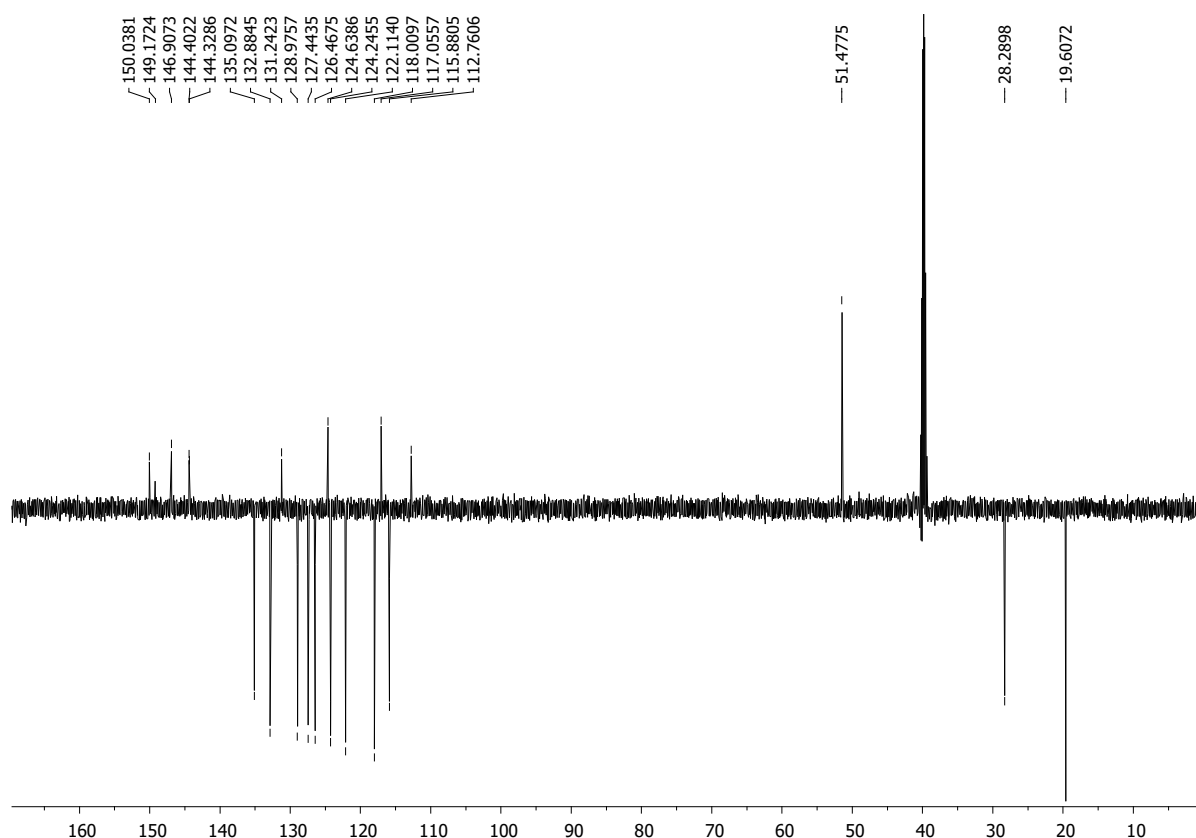


**Figure S24.**  $^{13}\text{C}$  NMR spectrum (DMSO- $d_6$ , 75 MHz) of 7-(*N*-isobutylamino)benzo[*g*]benzo[4,5]imidazo[1,2-*a*][1,8]naphthyridine-6-carbonitrile **7**

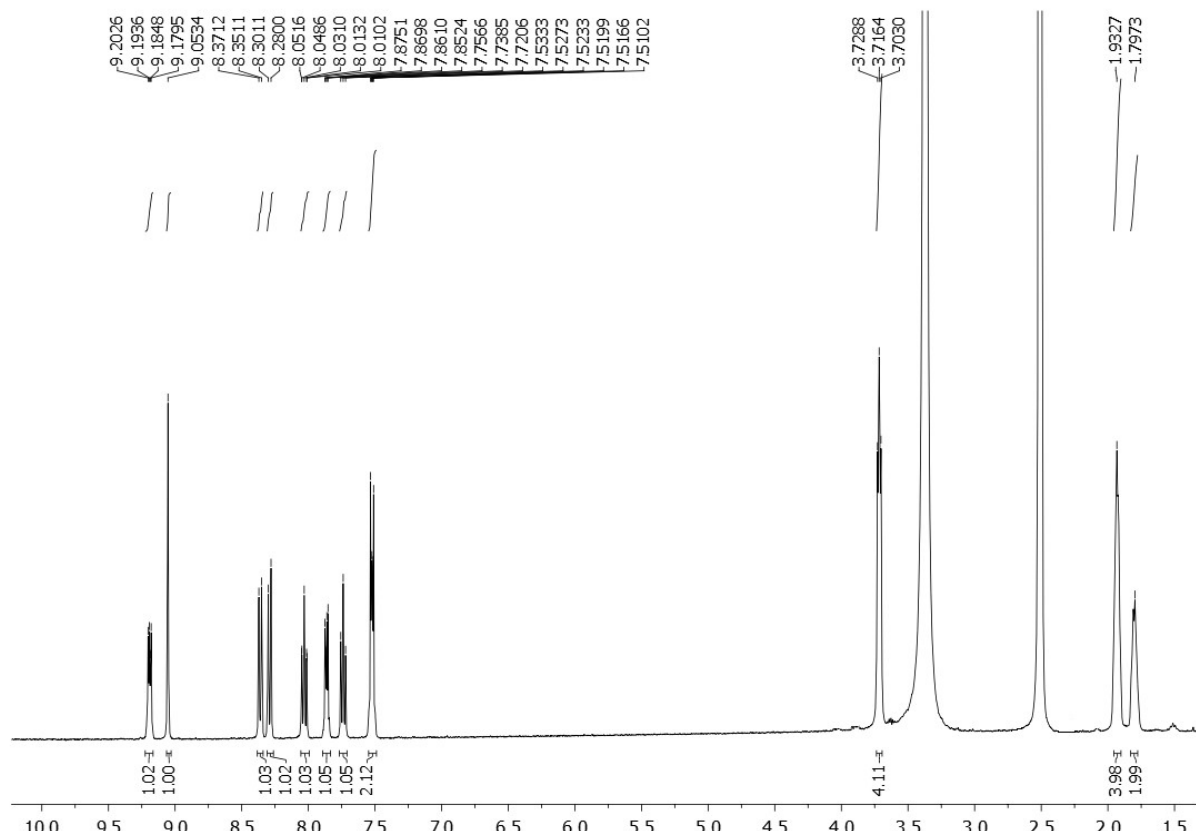


**Figure S25.**  $^1\text{H}$  NMR spectrum (DMSO- $d_6$ , 300 MHz) of 7-(piperidin-1-yl)benzo[*g*]benzo[4,5]imidazo[1,2-*a*][1,8]naphthyridine-6-carbonitrile **8**

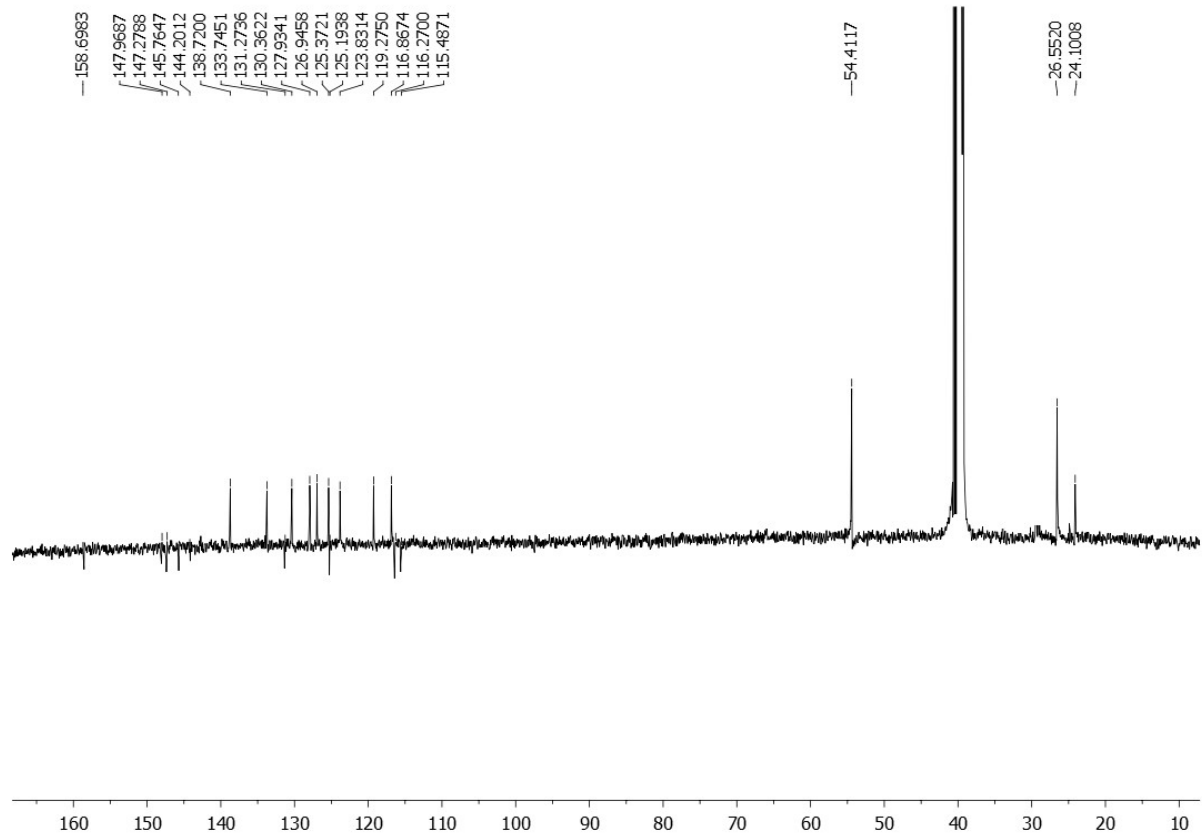


**Figure S26.**  $^{13}\text{C}$  NMR spectrum (DMSO- $d_6$ , 75 MHz) of 7-(piperidin-1-yl)benzo[*g*]benzo[4,5]imidazo[1,2-*a*][1,8]naphthyridine-6-carbonitrile **8**

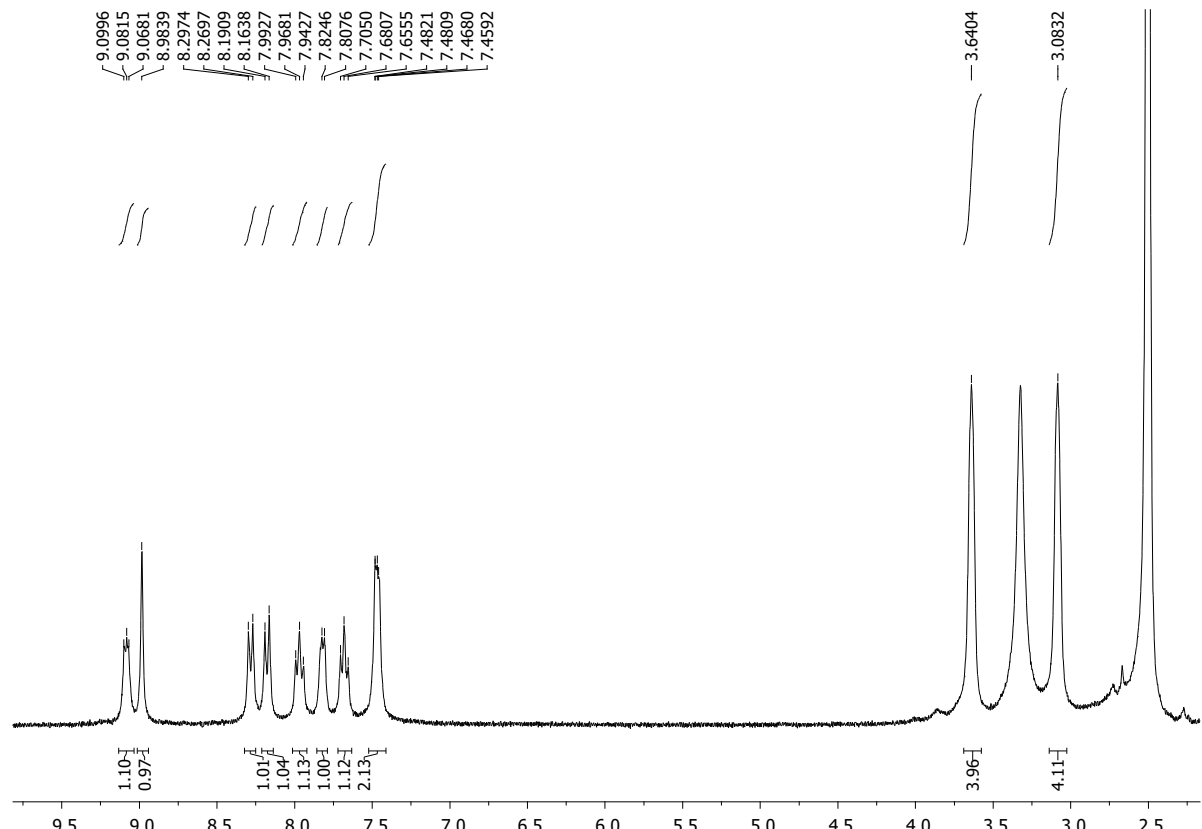


**Figure S27.**  $^1\text{H}$  NMR spectrum (DMSO- $d_6$ , 300 MHz) of 7-(piperazin-1-yl)benzo[*g*]benzo[4,5]imidazo[1,2-*a*][1,8]naphthyridine-6-carbonitrile **9**

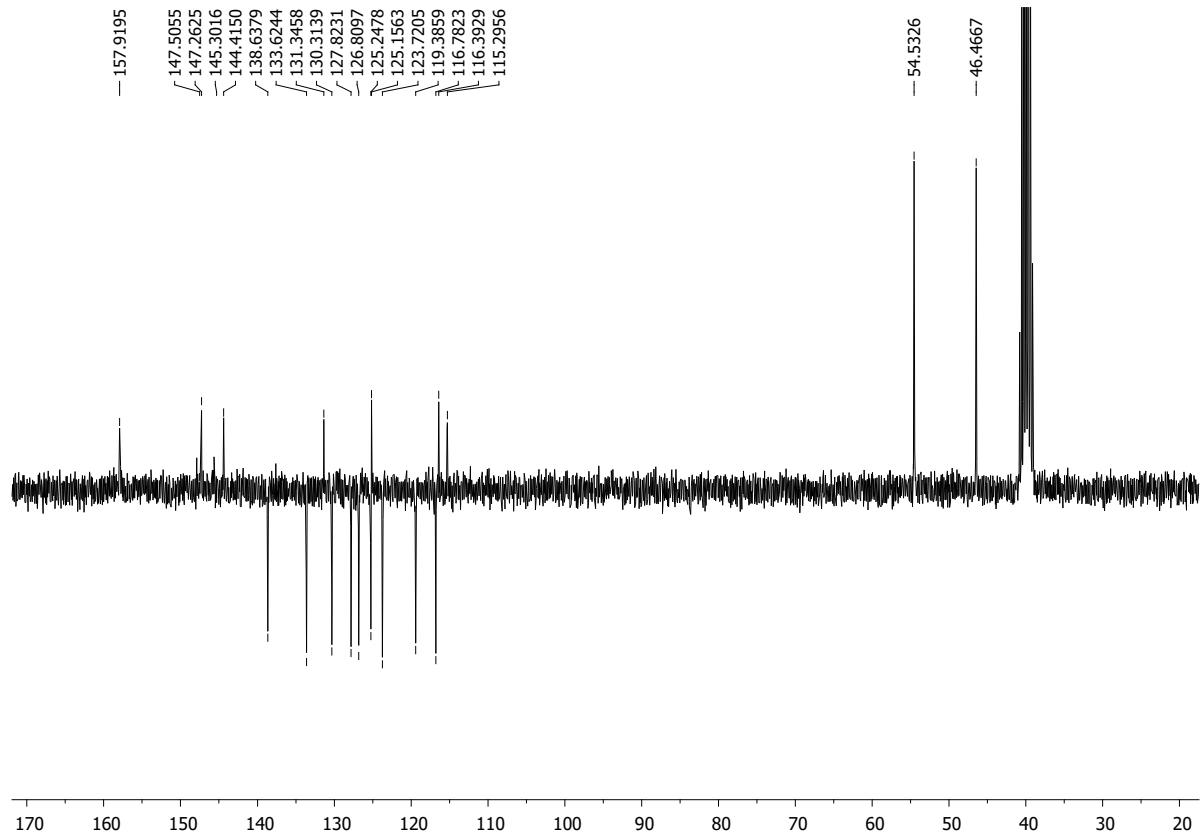


**Figure S28.**  $^{13}\text{C}$  NMR spectrum (DMSO- $d_6$ , 75 MHz) of 7-(piperazin-1-yl)benzo[*g*]benzo[4,5]imidazo[1,2-*a*][1,8]naphthyridine-6-carbonitrile **9**

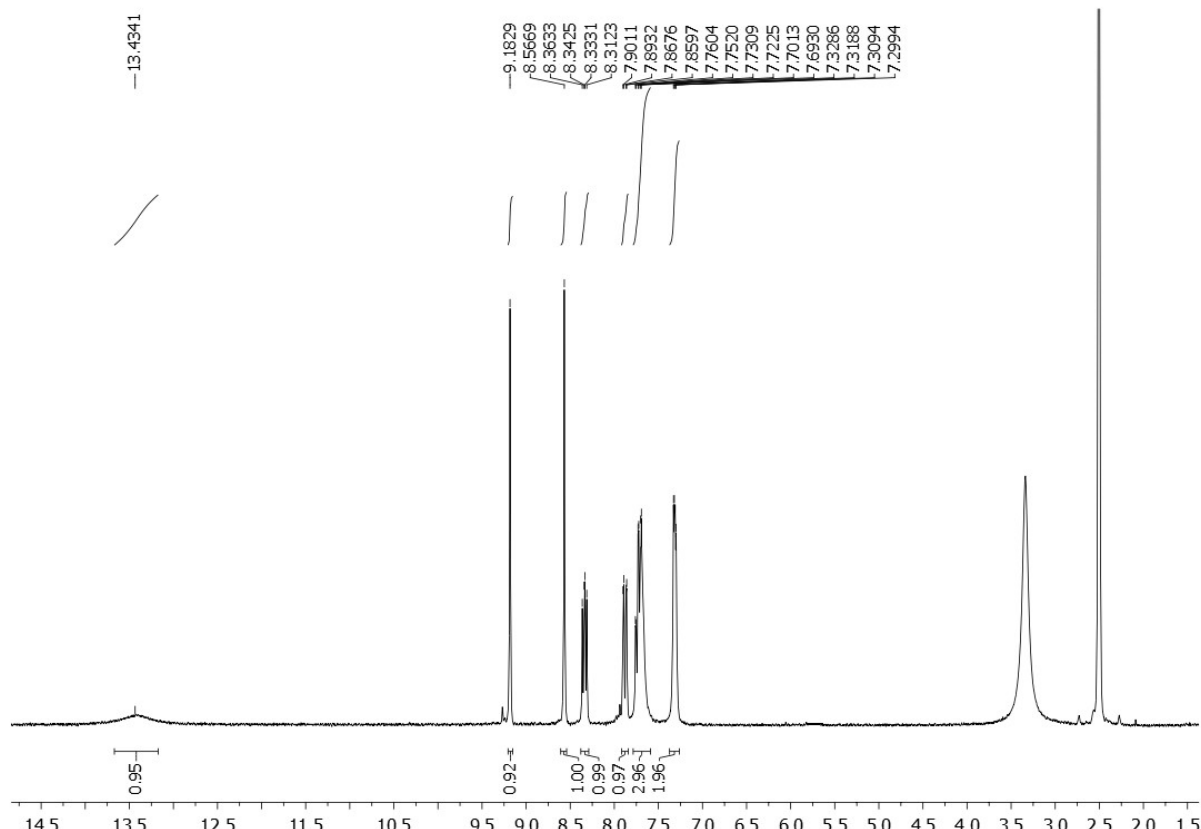


**Figure S29.**  $^1\text{H}$  NMR spectrum (DMSO- $d_6$ , 300 MHz) of (*E*)-2-(1*H*-benzo[*d*]imidazol-2-yl)-3-(2-chloro-7-fluoroquinolin-3-yl)acrylonitrile **13**

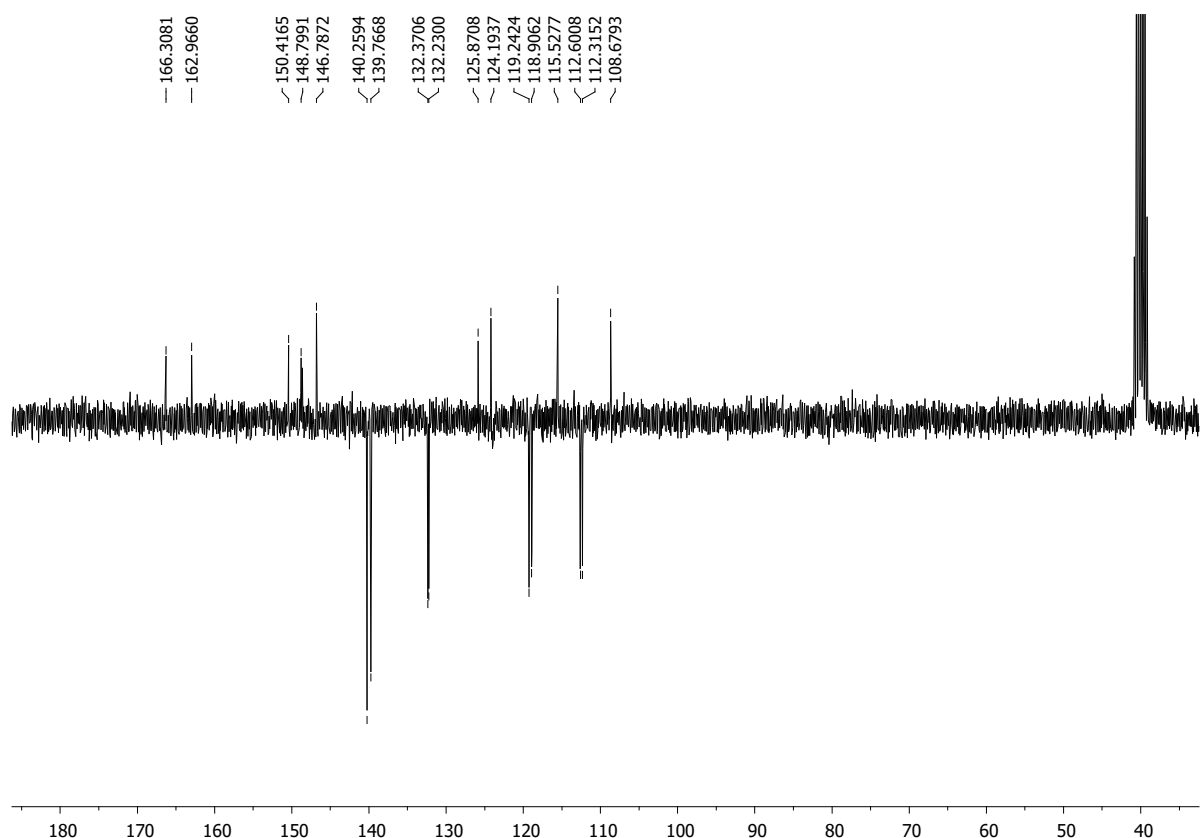


**Figure S30.**  $^{13}\text{C}$  NMR spectrum (DMSO- $d_6$ , 75 MHz) of (*E*)-2-(1*H*-benzo[*d*]imidazol-2-yl)-3-(2-chloro-7-fluoroquinolin-3-yl)acrylonitrile **13**

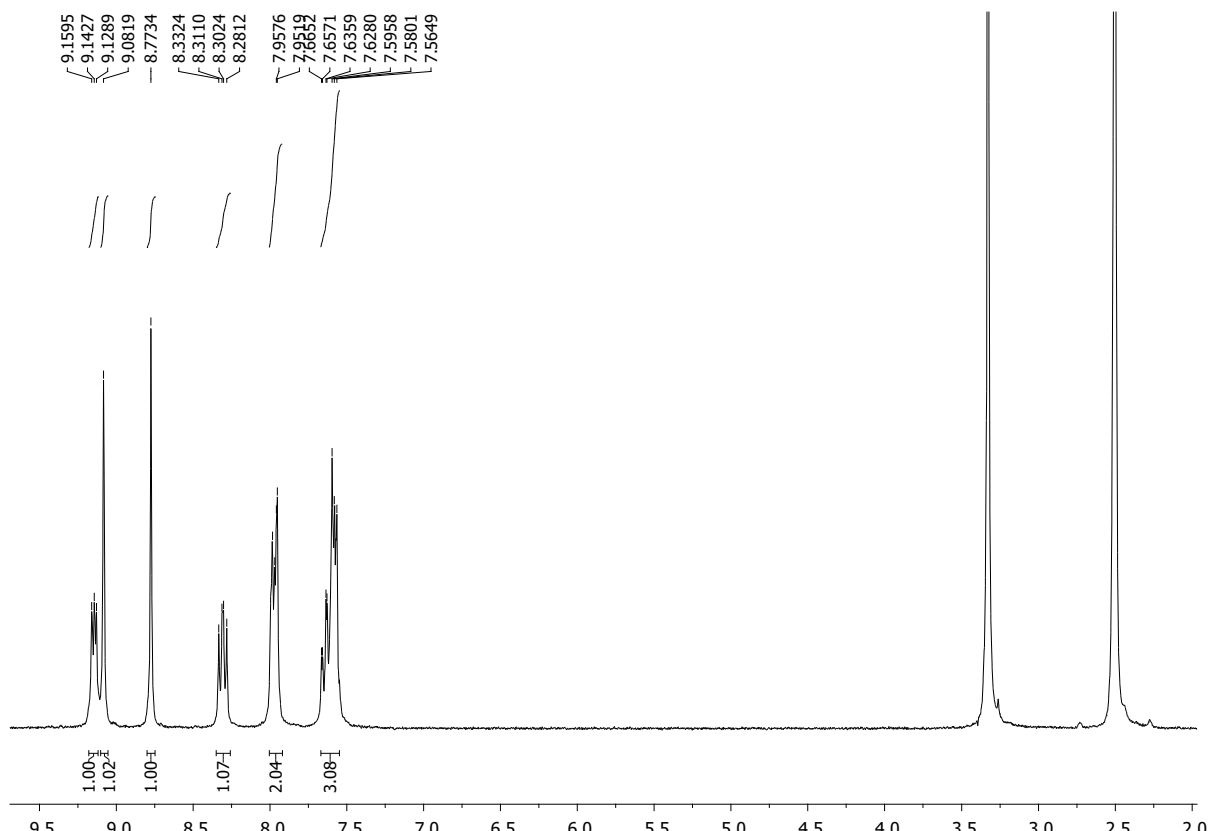


**Figure S31.**  $^1\text{H}$  NMR spectrum (DMSO- $d_6$ , 300 MHz) of 11-fluorobenzo[*g*]benzo[4,5]imidazo[1,2-*a*][1,8]naphthyridine-6-carbonitrile **16**

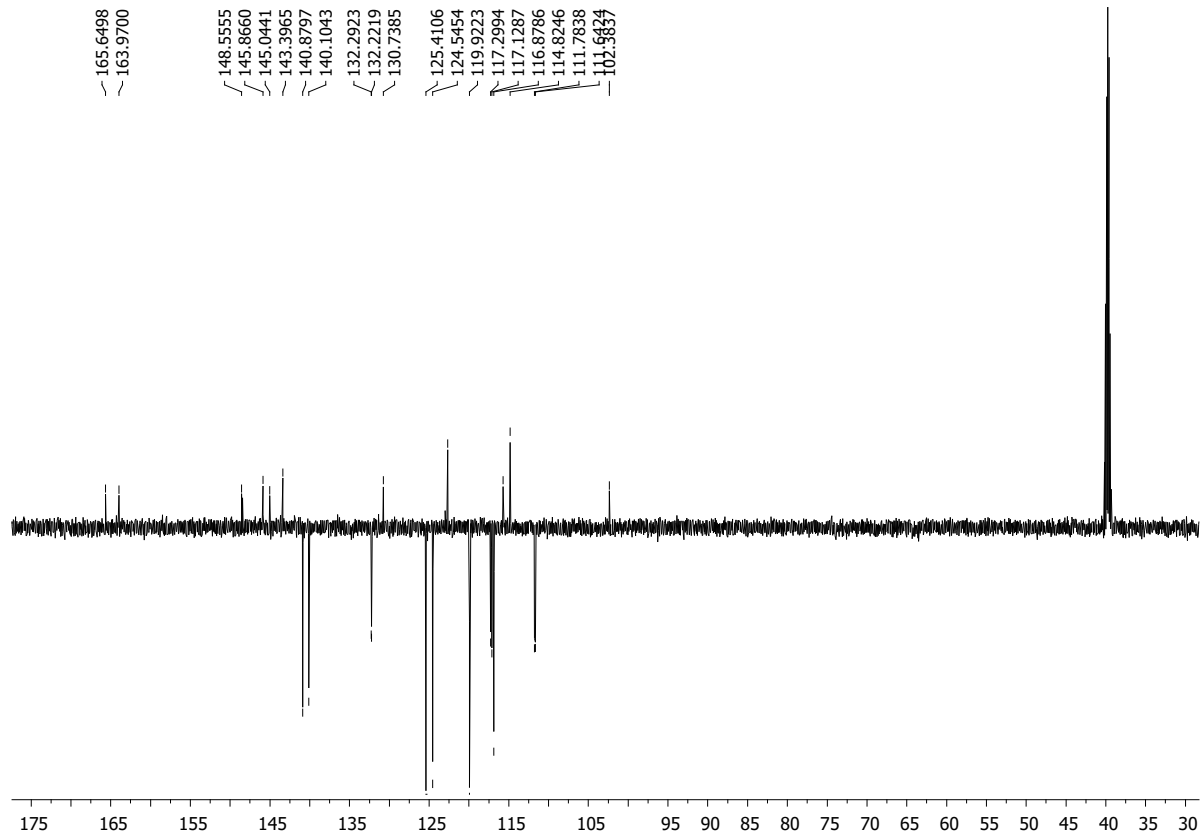


**Figure S32.**  $^{13}\text{C}$  NMR spectrum (DMSO- $d_6$ , 75 MHz) of 11-fluorobenzo[*g*]benzo[4,5]imidazo[1,2-*a*][1,8]naphthyridine-6-carbonitrile **16**

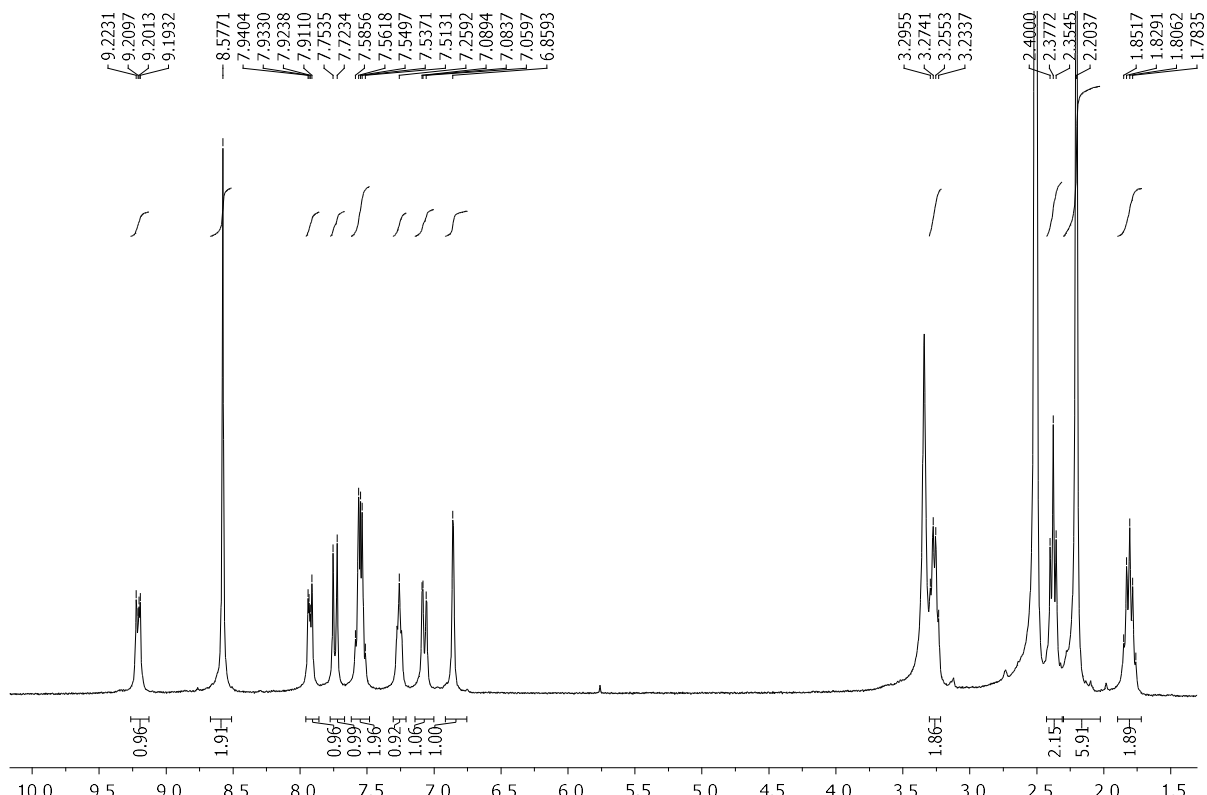


**Figure S33.**  $^1\text{H}$  NMR spectrum (DMSO- $d_6$ , 300 MHz) of 11-((3-*N,N*-dimethylamino)propyl)amino)benzo[*g*]benzo[4,5]imidazo[1,2-*a*][1,8]naphthyridine-6-carbonitrile **19**

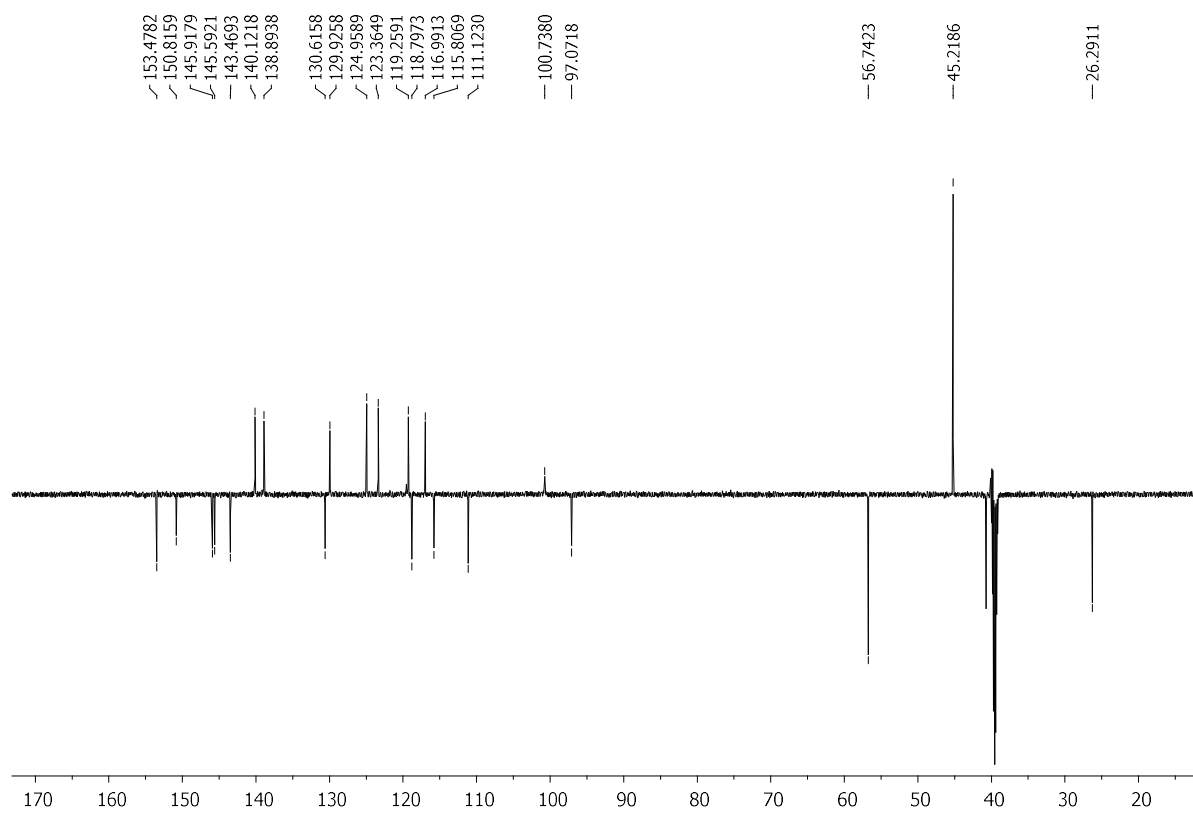


**Figure S34.**  $^{13}\text{C}$  NMR spectrum (DMSO- $d_6$ , 150 MHz) of 11-((3-*N,N*-dimethylamino)propyl)amino)benzo[*g*]benzo[4,5]imidazo[1,2-*a*][1,8]naphthyridine-6-carbonitrile **19**

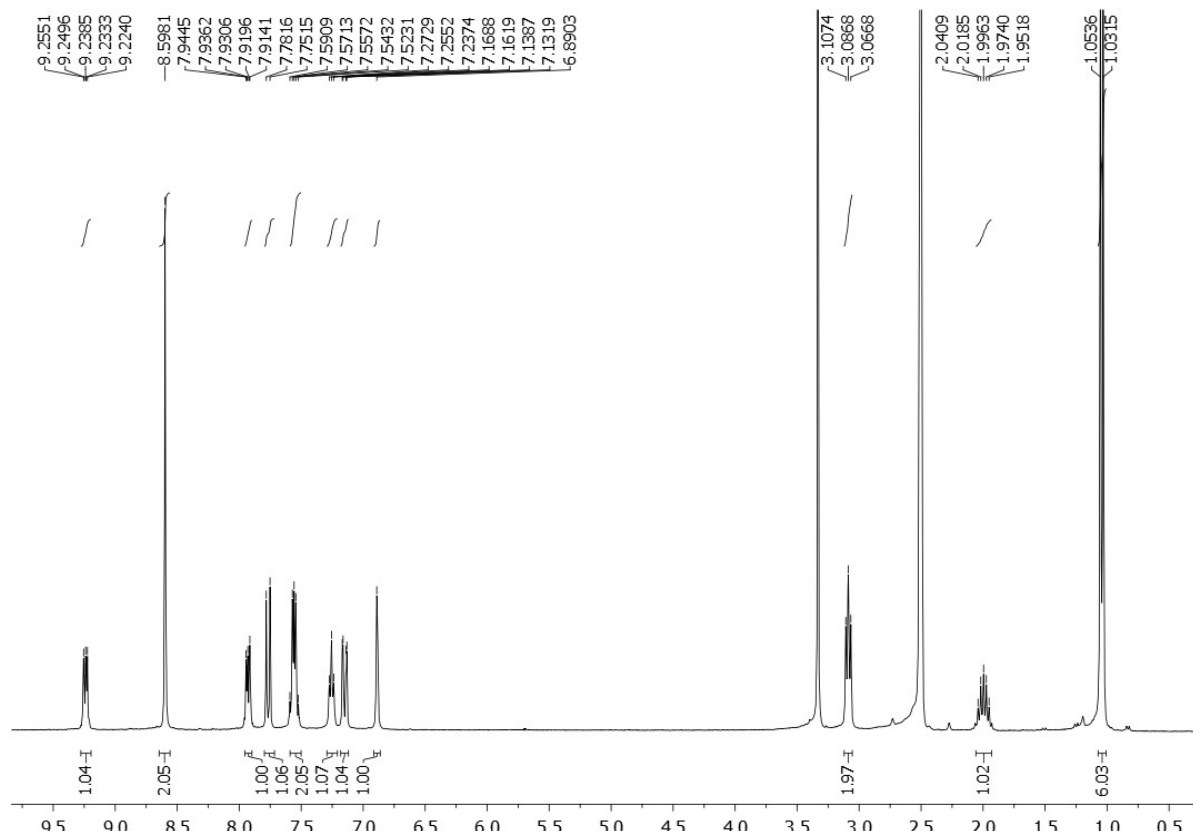


**Figure S35.**  $^1\text{H}$  NMR spectrum (DMSO- $d_6$ , 300 MHz) of 11-(*N*-isobutylamino)benzo[*g*]benzo[4,5]imidazo[1,2-*a*][1,8]naphthyridine-6-carbonitrile **20**

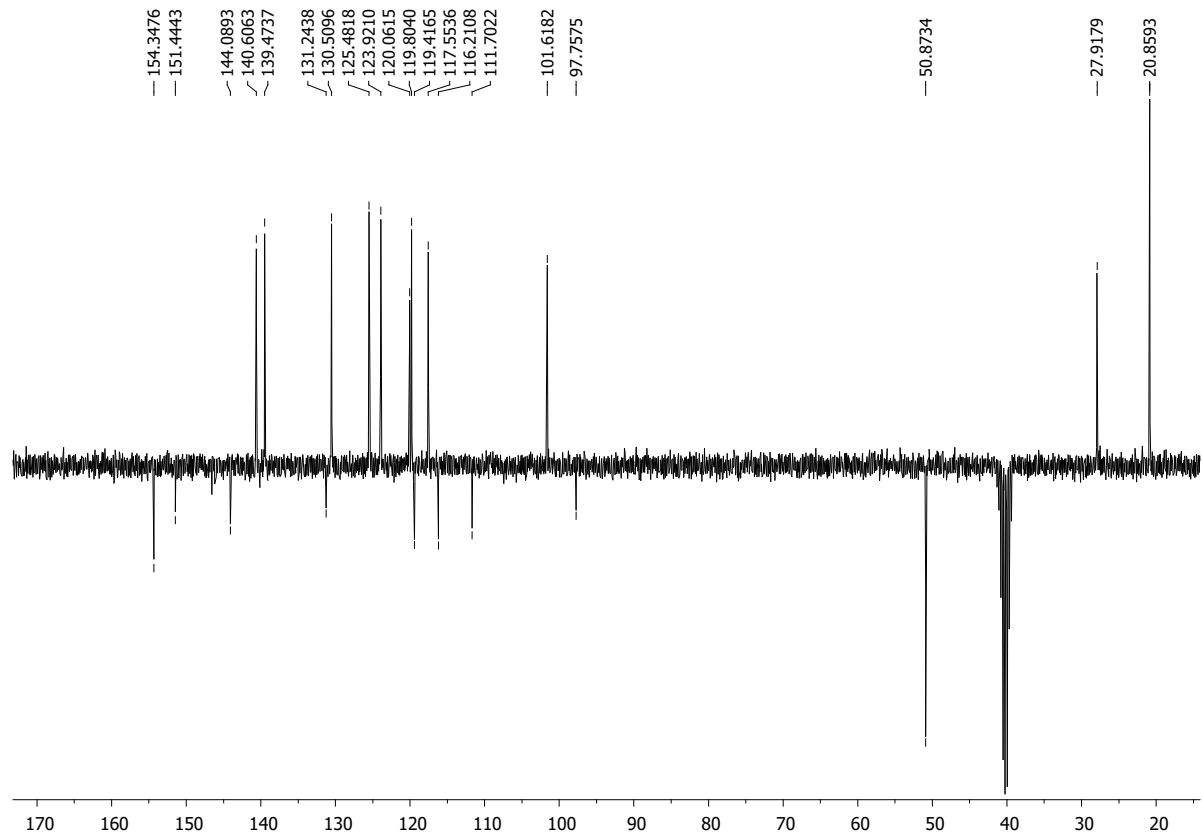


**Figure S36.**  $^{13}\text{C}$  NMR spectrum (DMSO- $d_6$ , 75 MHz) of 11-(*N*-isobutylamino)benzo[*g*]benzo[4,5]imidazo[1,2-*a*][1,8]naphthyridine-6-carbonitrile **20**

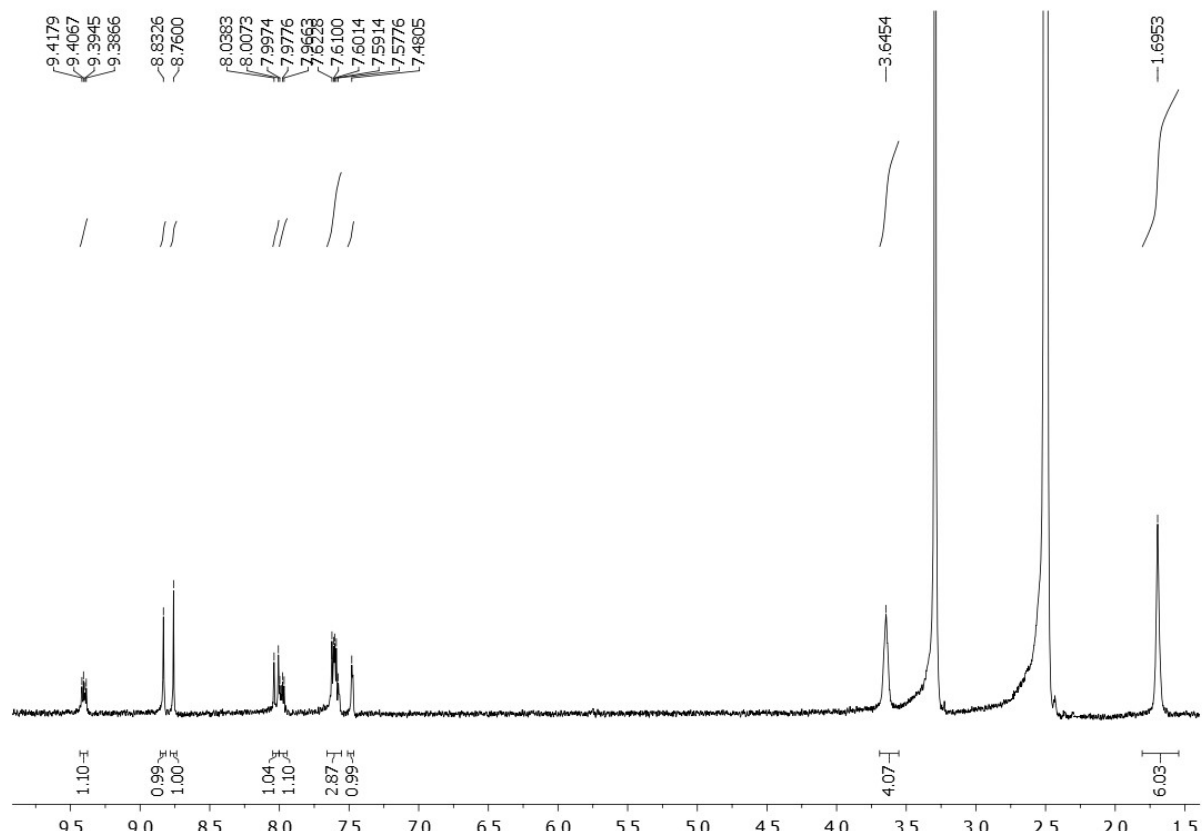


**Figure S37.**  $^1\text{H}$  NMR spectrum (DMSO- $d_6$ , 300 MHz) of 11-(piperidin-1-yl)benzo[*g*]benzo[4,5]imidazo[1,2-*a*][1,8]naphthyridine-6-carbonitrile **21**

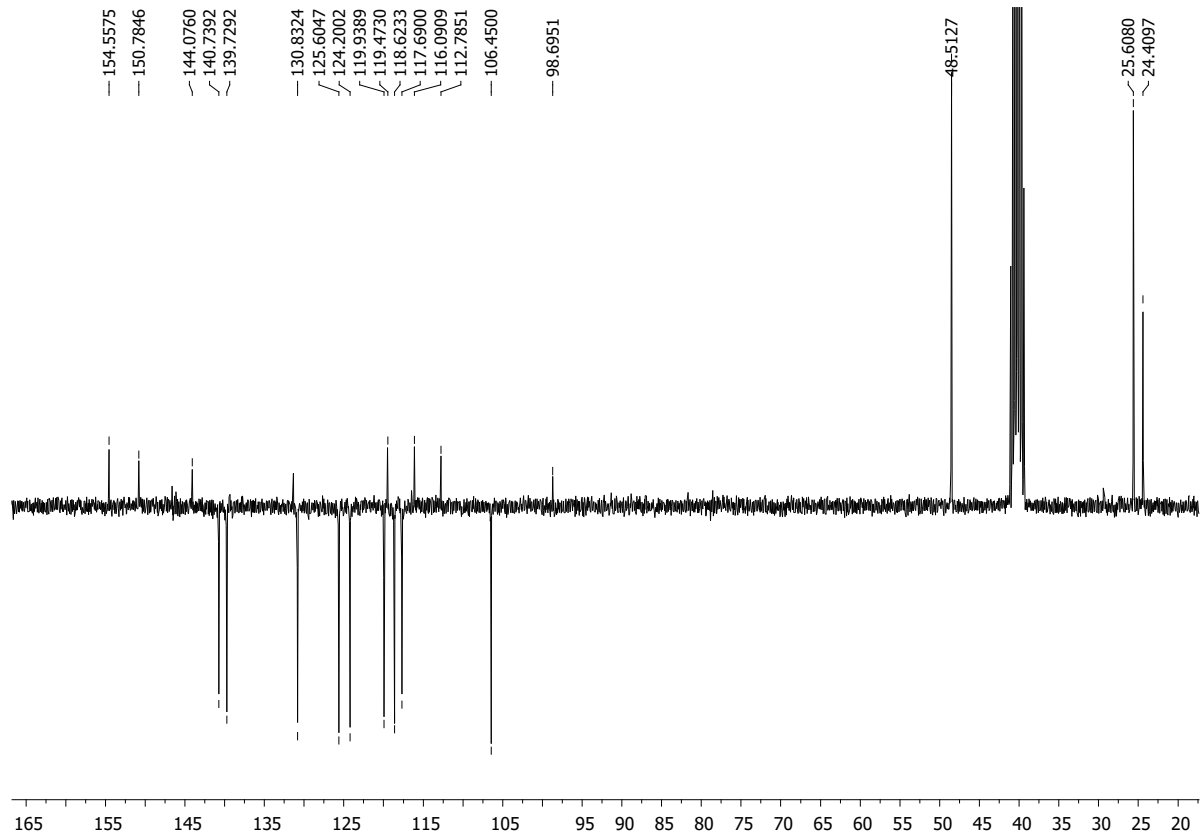


**Figure S38.**  $^{13}\text{C}$  NMR spectrum (DMSO- $d_6$ , 75 MHz) of 11-(piperidin-1-yl)benzo[*g*]benzo[4,5]imidazo[1,2-*a*][1,8]naphthyridine-6-carbonitrile **21**

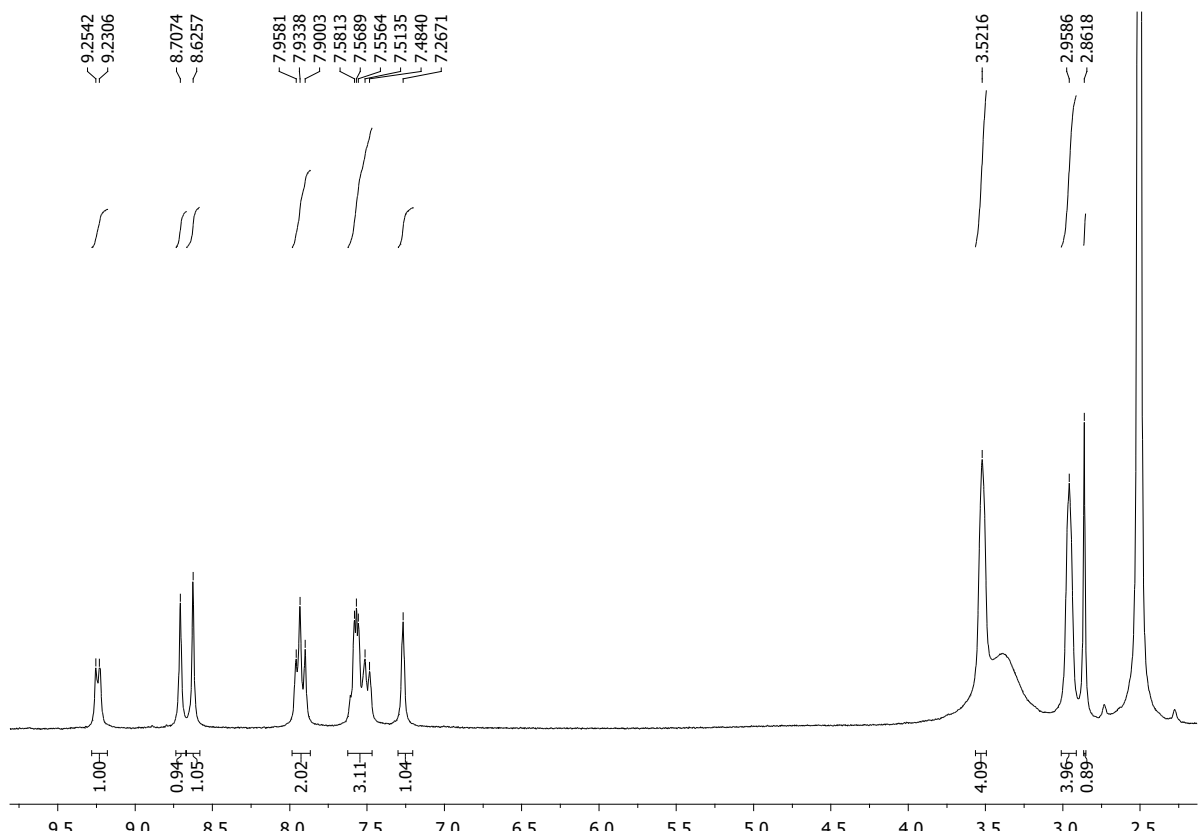


**Figure S39.**  $^1\text{H}$  NMR spectrum (DMSO- $d_6$ , 300 MHz) of 11-(piperazin-1-yl)benzo[*g*]benzo[4,5]imidazo[1,2-*a*][1,8]naphthyridine-6-carbonitrile **22**

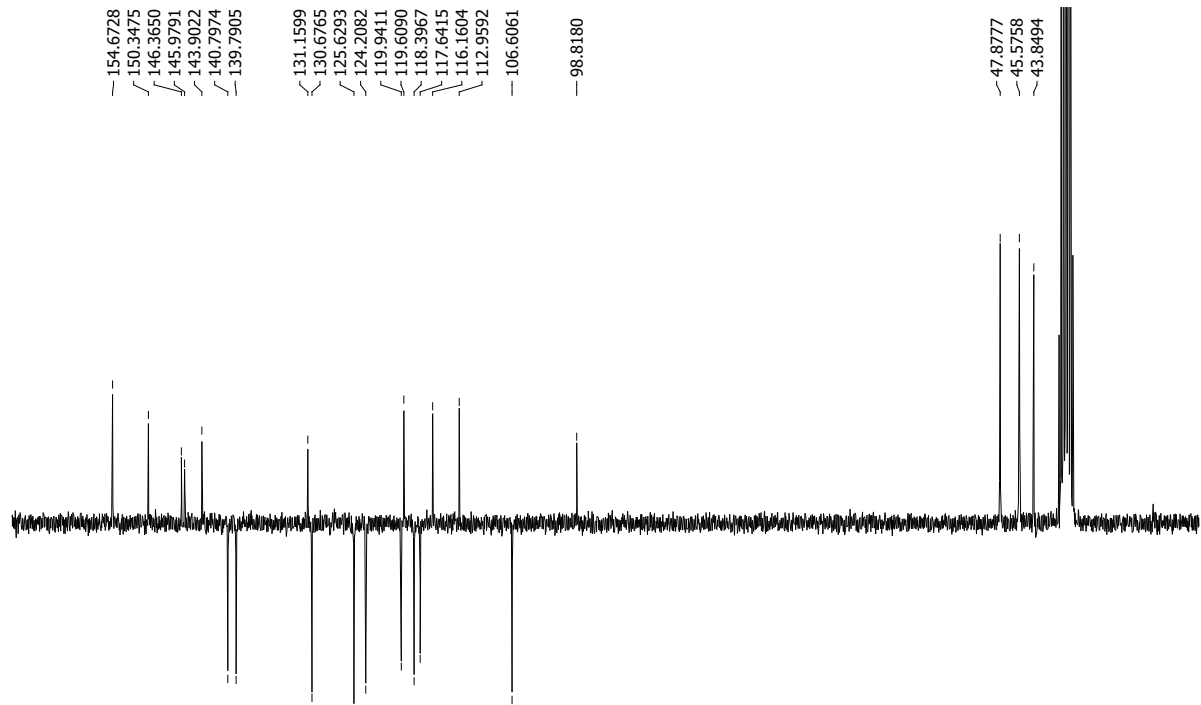


**Figure S40.** <sup>13</sup>C NMR spectrum (DMSO-*d*<sub>6</sub>, 75 MHz) of 11-(piperazin-1-yl)benzo[*g*]benzo[4,5]imidazo[1,2-*a*][1,8]naphthyridine-6-carbonitrile **22**

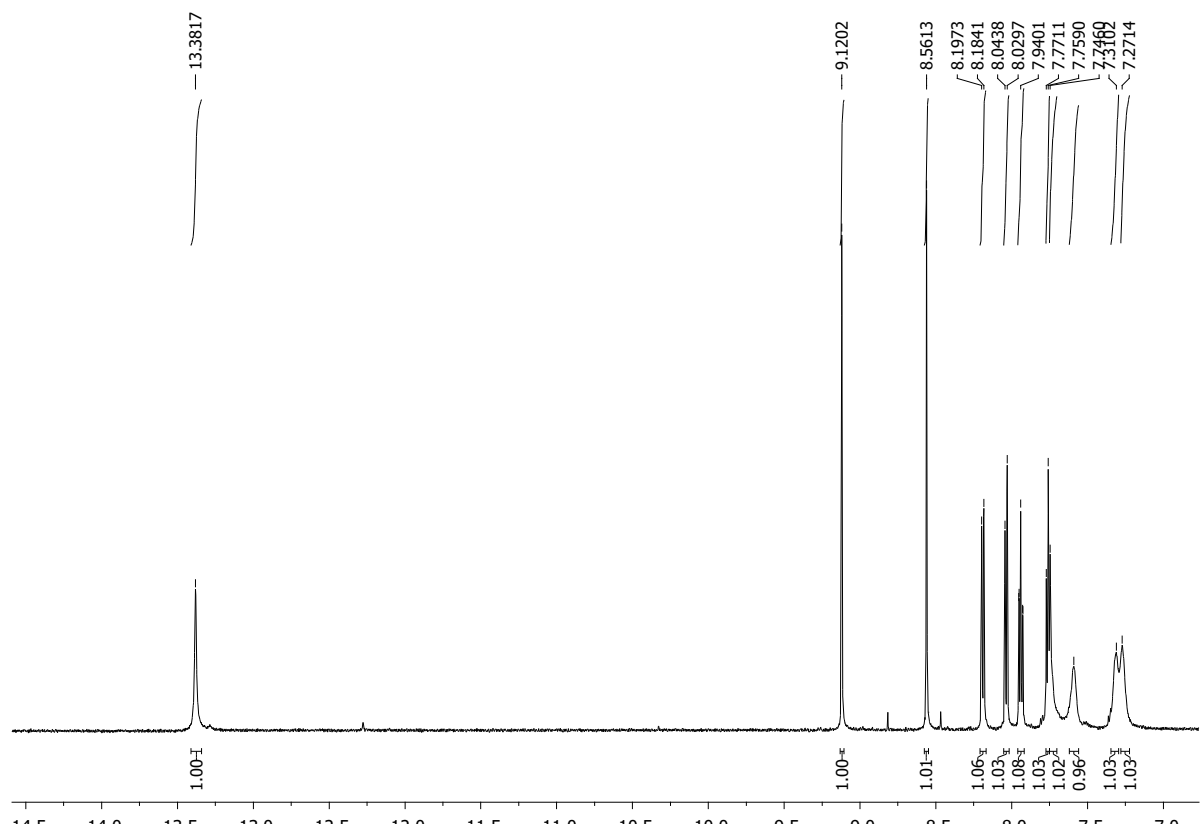


**Figure S41.** <sup>1</sup>H NMR spectrum (DMSO-*d*<sub>6</sub>, 600 MHz) of (*E*)-2-(1*H*-benzo[*d*]imidazol-2-yl)-3-(2-chloroquinolin-3-yl)acrylonitrile **14**

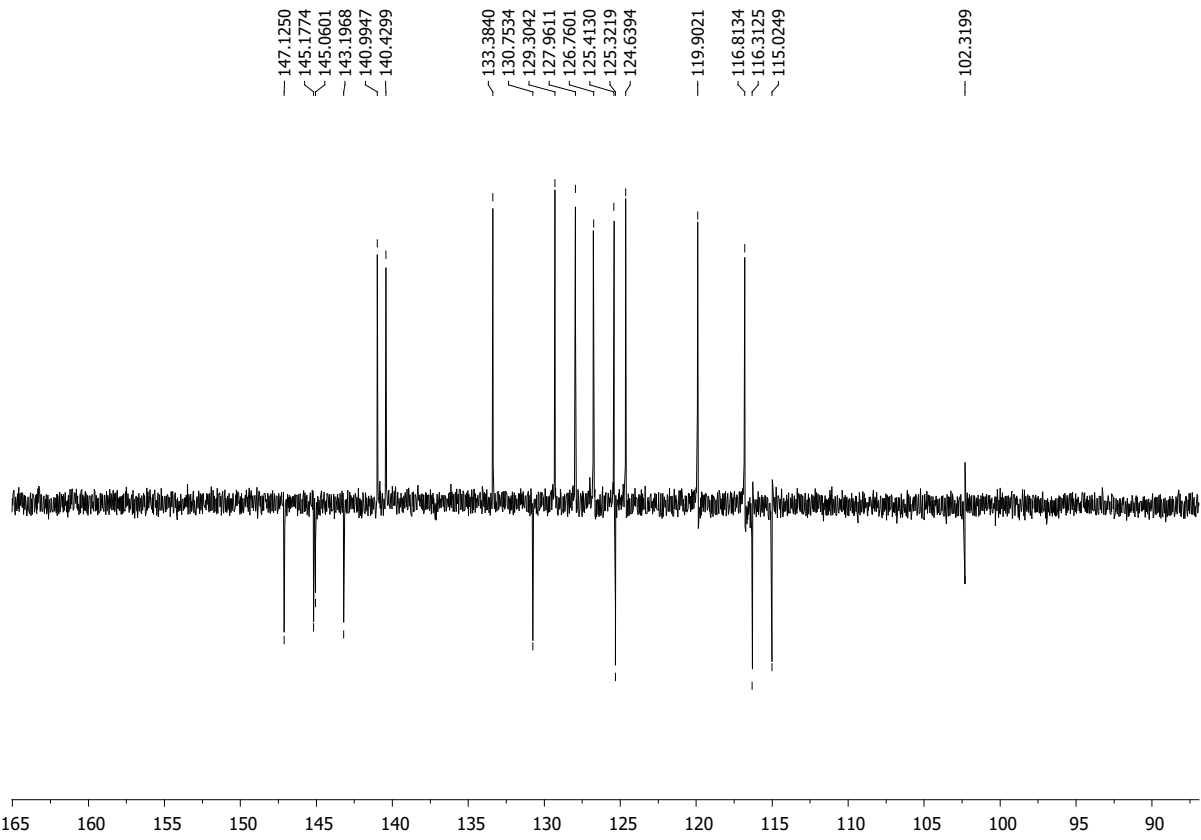


**Figure S42.**  $^{13}\text{C}$  NMR spectrum (DMSO- $d_6$ , 150 MHz) of (*E*)-2-(1*H*-benzo[*d*]imidazol-2-yl)-3-(2-chloroquinolin-3-yl)acrylonitrile **14**

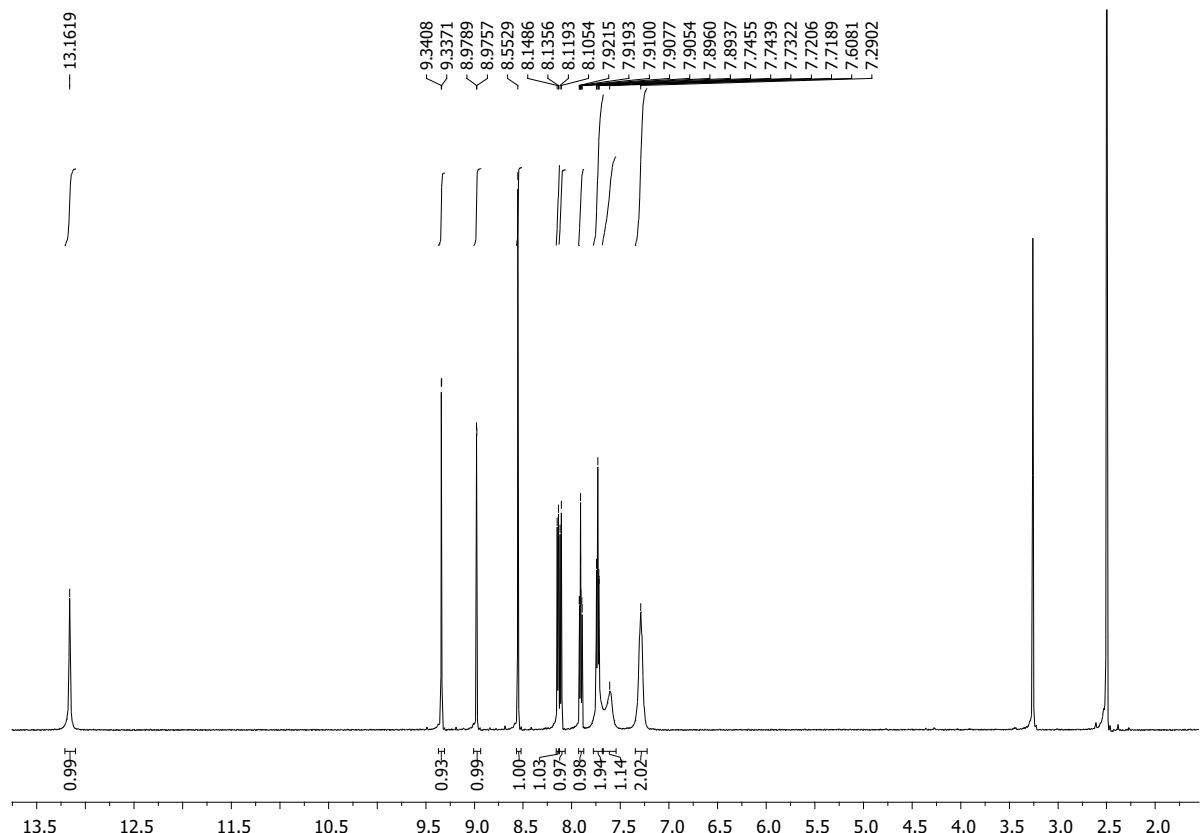


**Figure S43.**  $^1\text{H}$  NMR spectrum (DMSO- $d_6$ , 600 MHz) of (*E*)-2-(1*H*-benzo[*d*]imidazol-2-yl)-3-(quinolin-3-yl)acrylonitrile **15**

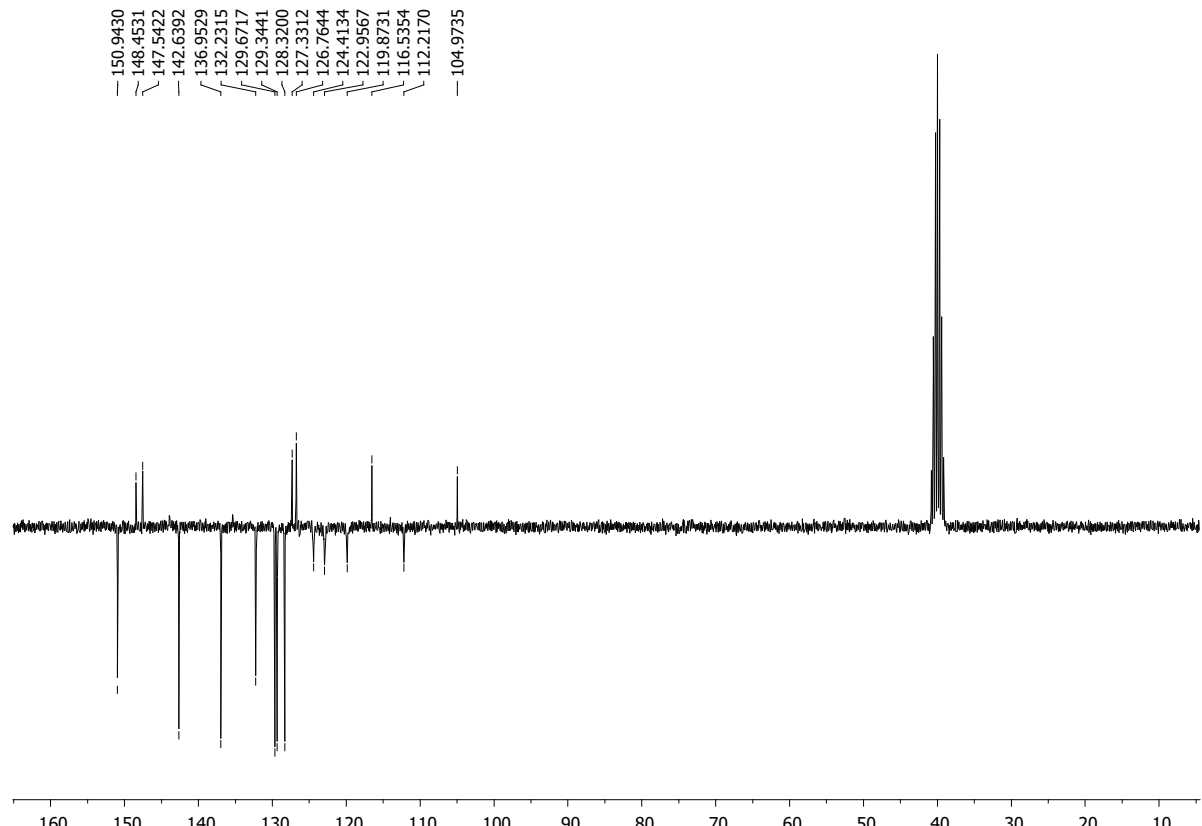


**Figure S44.** <sup>13</sup>C NMR spectrum (DMSO-d<sub>6</sub>, 75 MHz) of (*E*)-2-(1*H*-benzo[*d*]imidazol-2-yl)-3-(quinolin-3-yl)acrylonitrile **15**

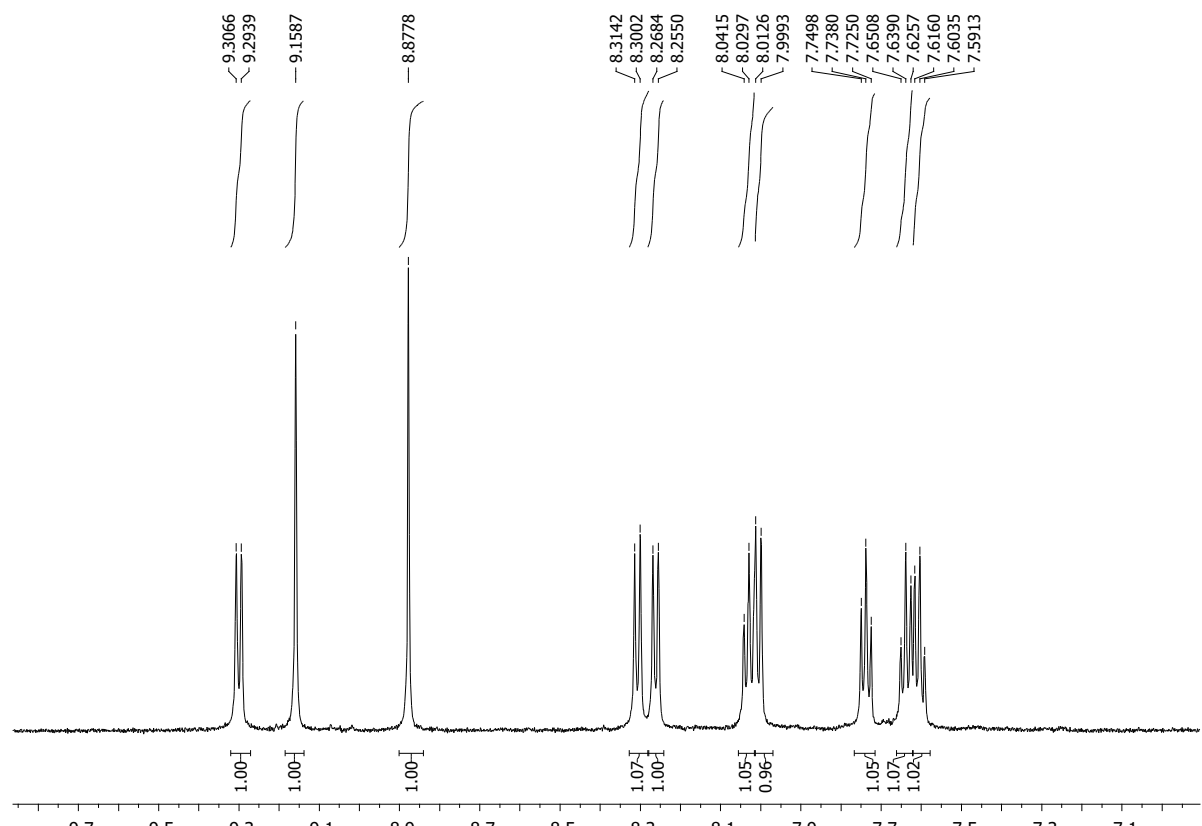


**Figure S45.** <sup>1</sup>H NMR spectrum (DMSO-d<sub>6</sub>, 600 MHz) of benzo[g]benzo[4,5]imidazo[1,2-*a*][1,8]naphthyridine-6-carbonitrile **17**

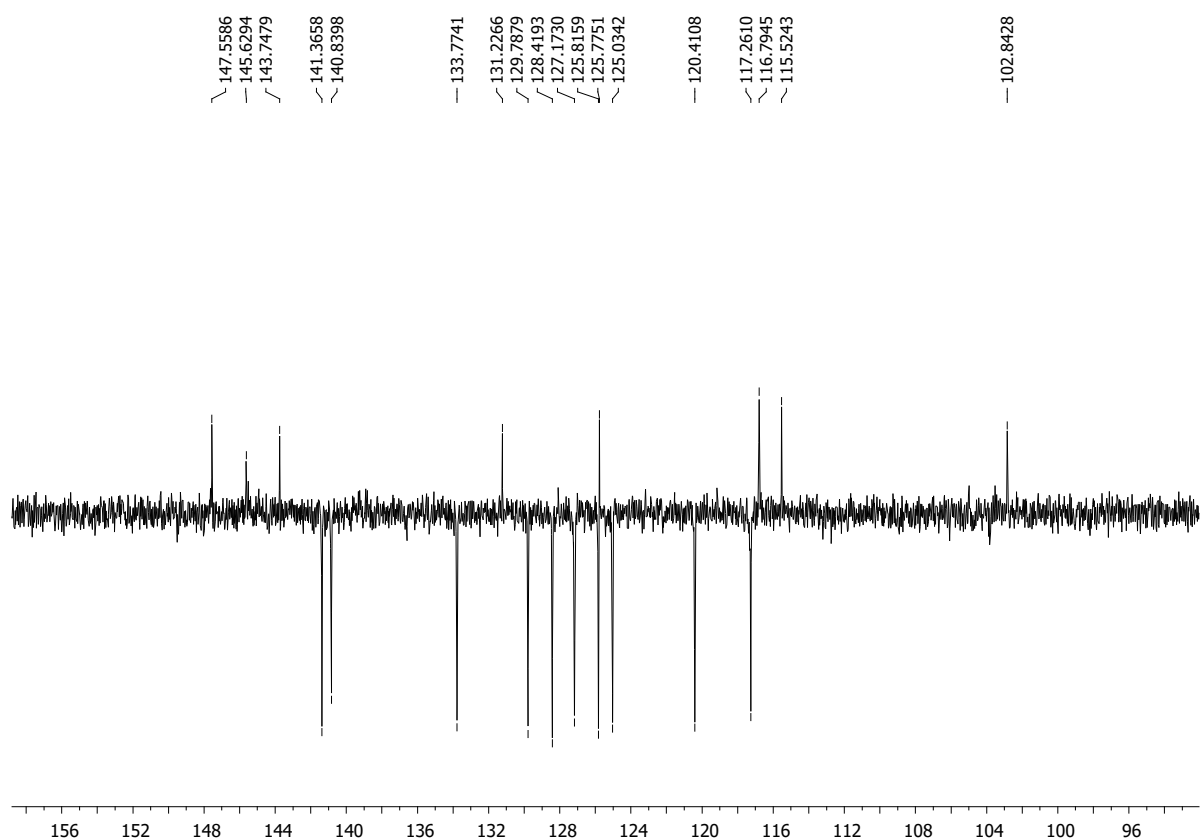


**Figure S46.**  $^{13}\text{C}$  NMR spectrum (DMSO- $d_6$ , 75 MHz) of *benzo[g]benzo[4,5]imidazo[1,2-a][1,8]naphthyridine-6-carbonitrile 17*

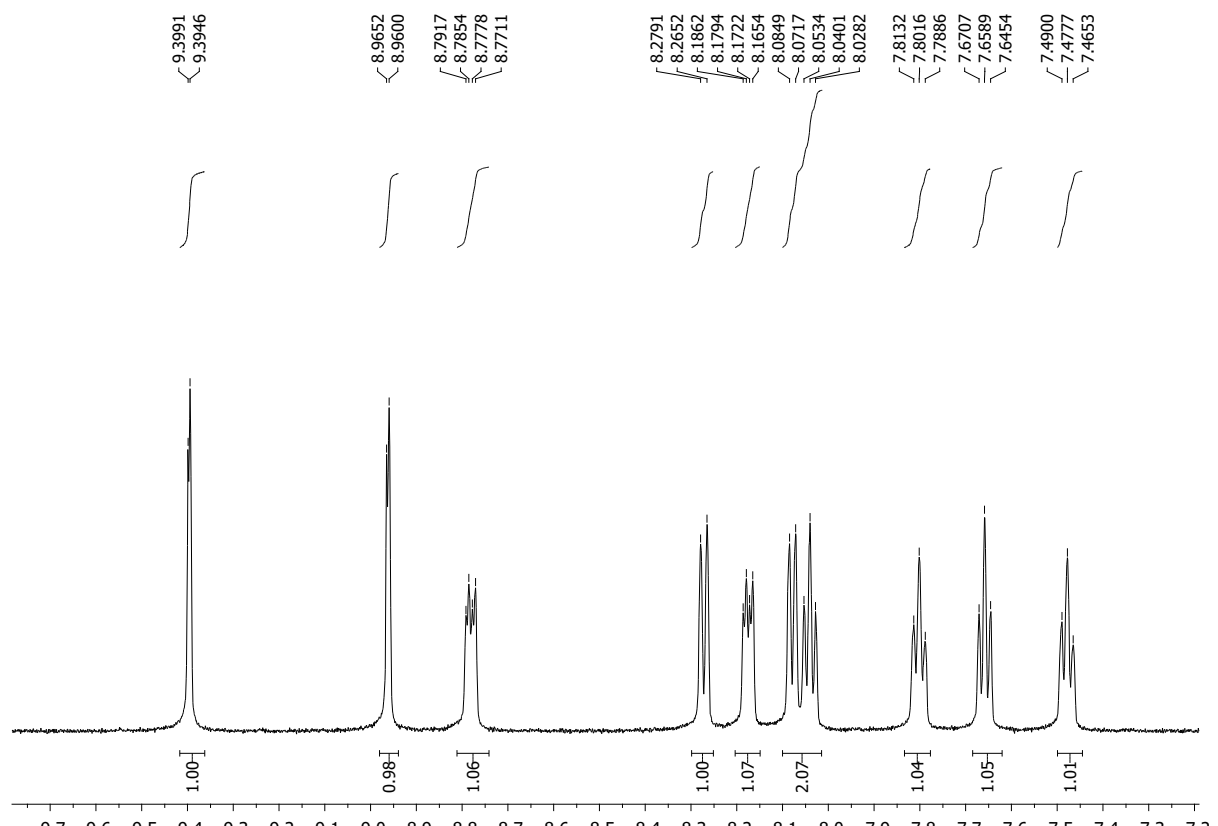


**Figure S47.**  $^1\text{H}$  NMR spectrum (DMSO- $d_6$ , 600 MHz) of *benzo[g]benzo[4,5]imidazo[1,2-a][1,5]naphthyridine-7-carbonitrile 18*

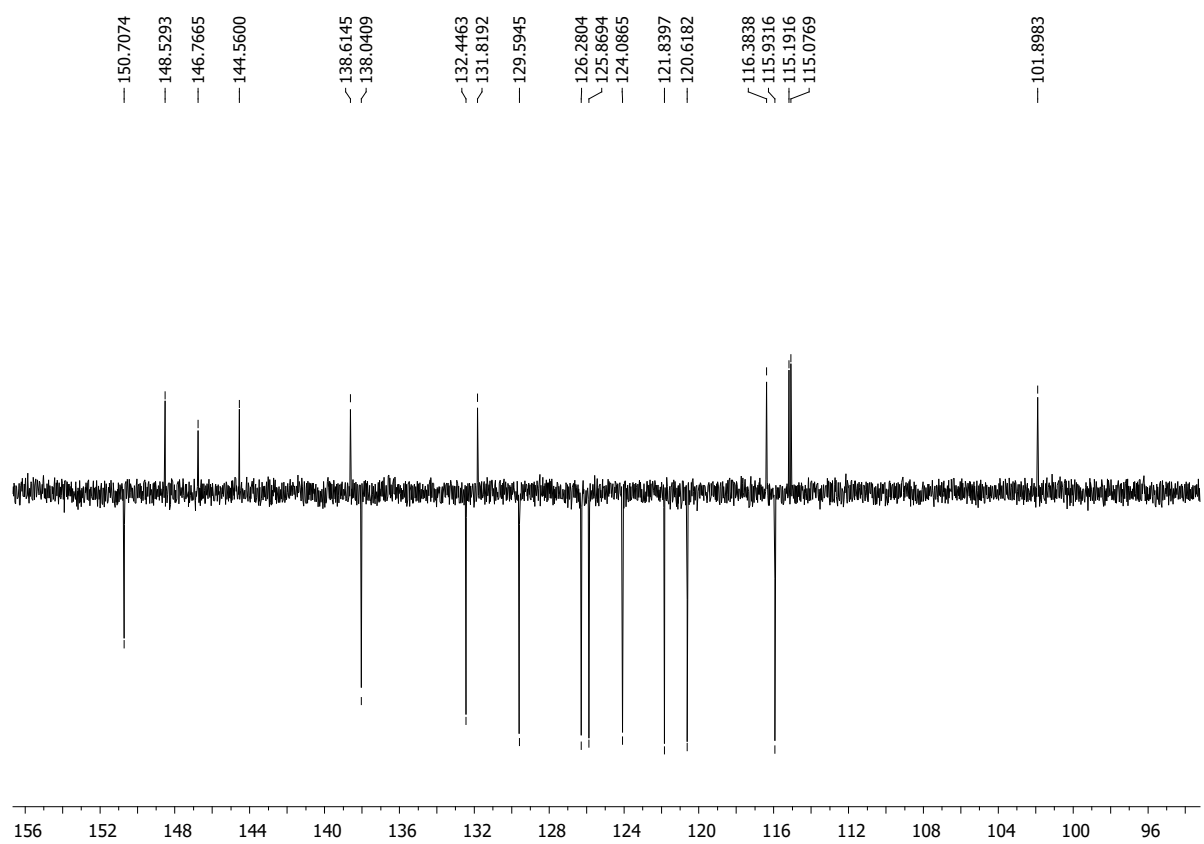


**Figure S48.**  $^{13}\text{C}$  NMR spectrum (DMSO- $d_6$ , 150 MHz) of *benzo[g]benzo[4,5]imidazo[1,2-a][1,5]naphthyridine-7-carbonitrile 18*

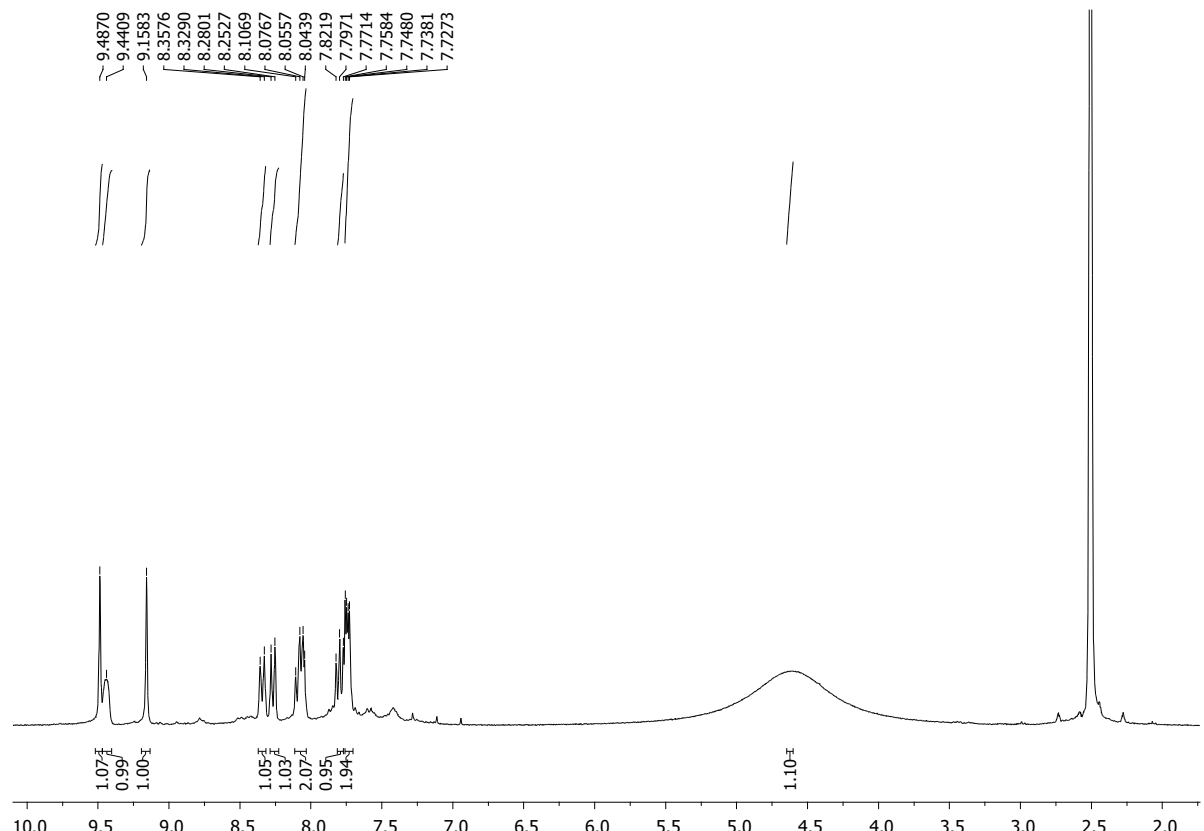


**Figure S49.**  $^1\text{H}$  NMR spectrum (DMSO- $d_6$ , 300 MHz) of *benzo[g]benzo[4,5]imidazo[1,2-a][1,8]naphthyridine-6-carboxylic acid 23*

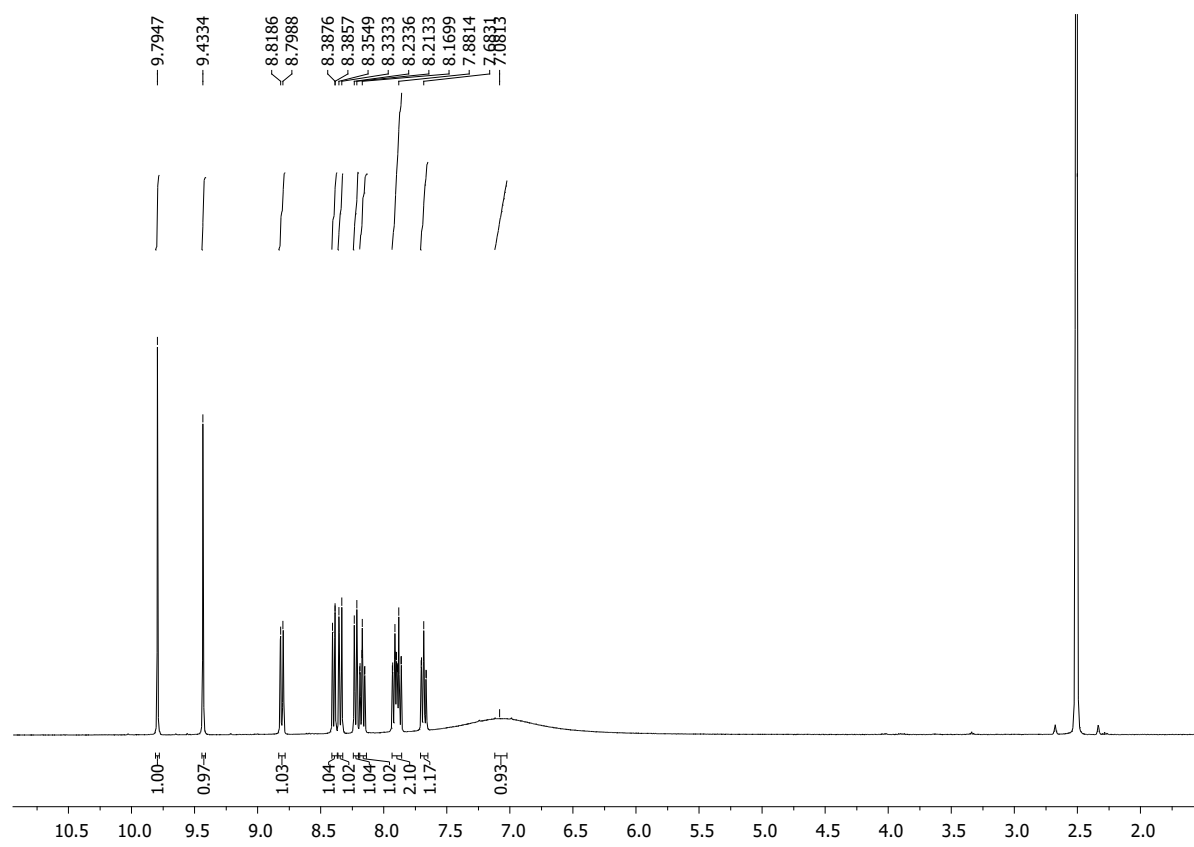


**Figure S50.**  $^1\text{H}$  NMR spectrum (DMSO- $d_6$ , 400 MHz) of *benzo[g]benzo[4,5]imidazo[1,2-a][1,5]naphthyridine-7-carboxylic acid 27*

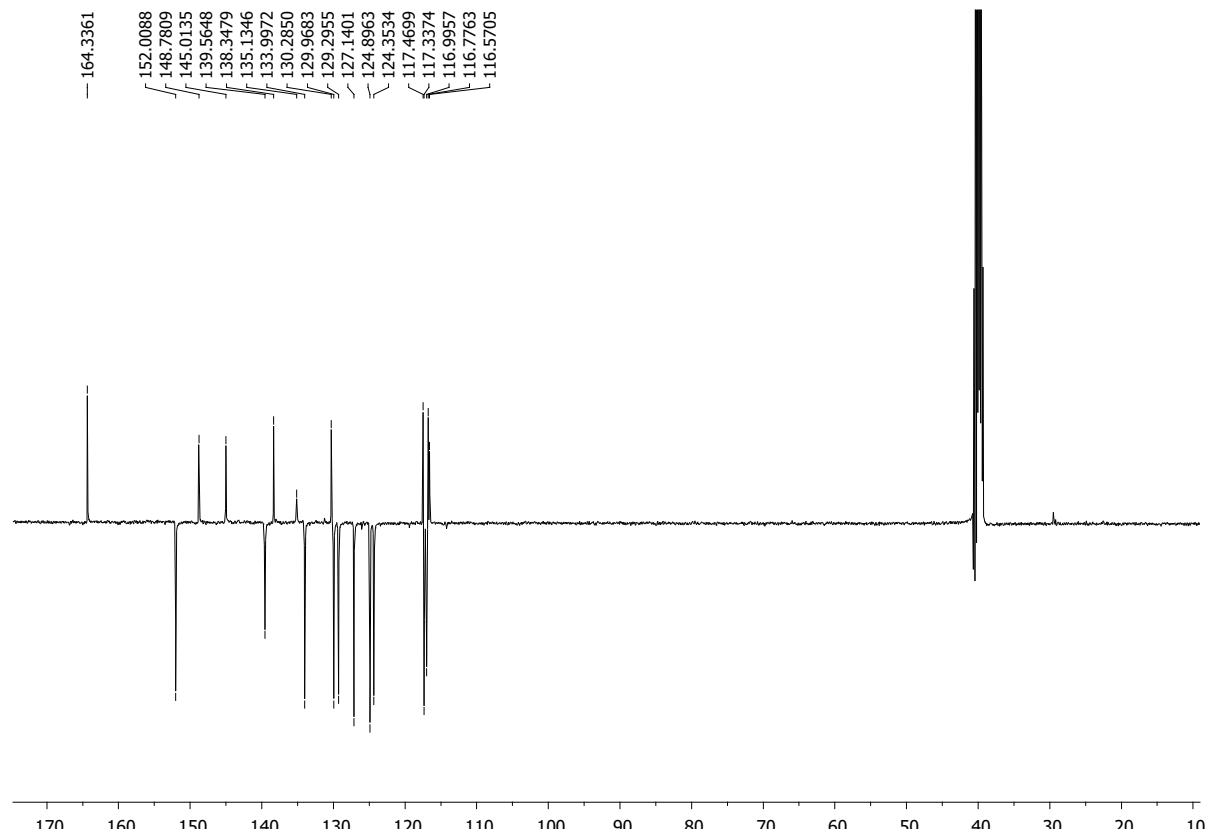


**Figure S51.**  $^{13}\text{C}$  NMR spectrum (DMSO- $d_6$ , 100 MHz) of *benzo[g]benzo[4,5]imidazo[1,2-a][1,5]naphthyridine-7-carboxylic acid 27*

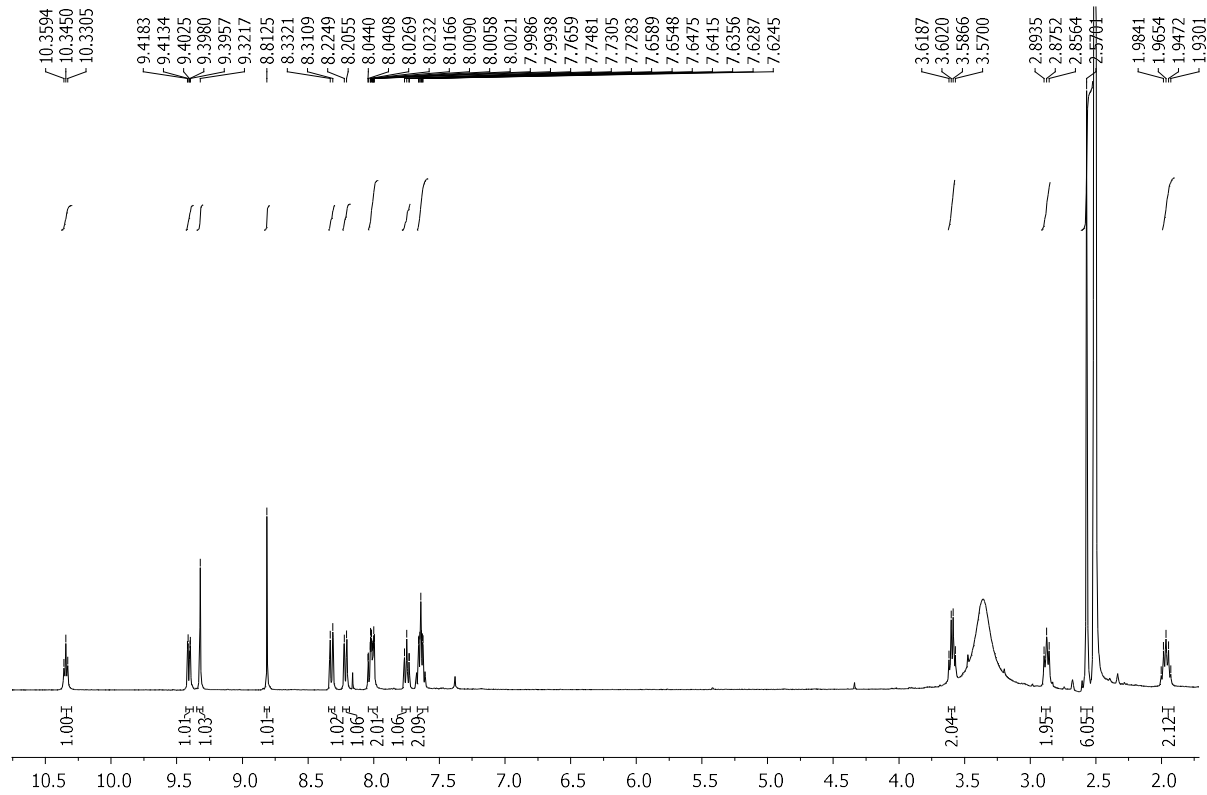


**Figure S52.**  $^1\text{H}$  NMR spectrum (DMSO- $d_6$ , 400 MHz) of *N*-(3-*N,N*-dimethylamino)propyl)benzo[*g*]benzo[4,5]imidazo[1,2-*a*][1,8]naphthyridine-6-carboxamide **25**

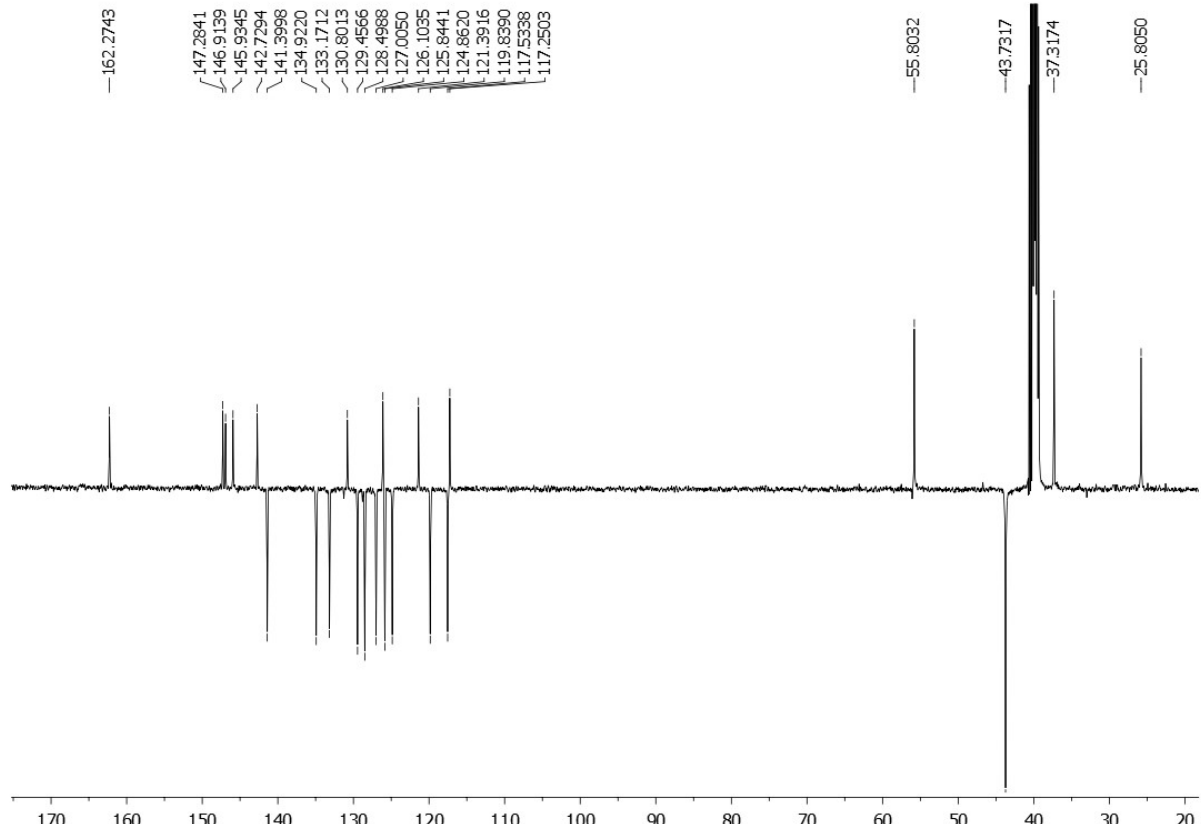


**Figure S53.**  $^{13}\text{C}$  NMR spectrum (DMSO- $d_6$ , 100 MHz) of *N*-(3-*N,N*-dimethylamino)propyl)benzo[*g*]benzo[4,5]imidazo[1,2-*a*][1,8]naphthyridine-6-carboxamide **25**

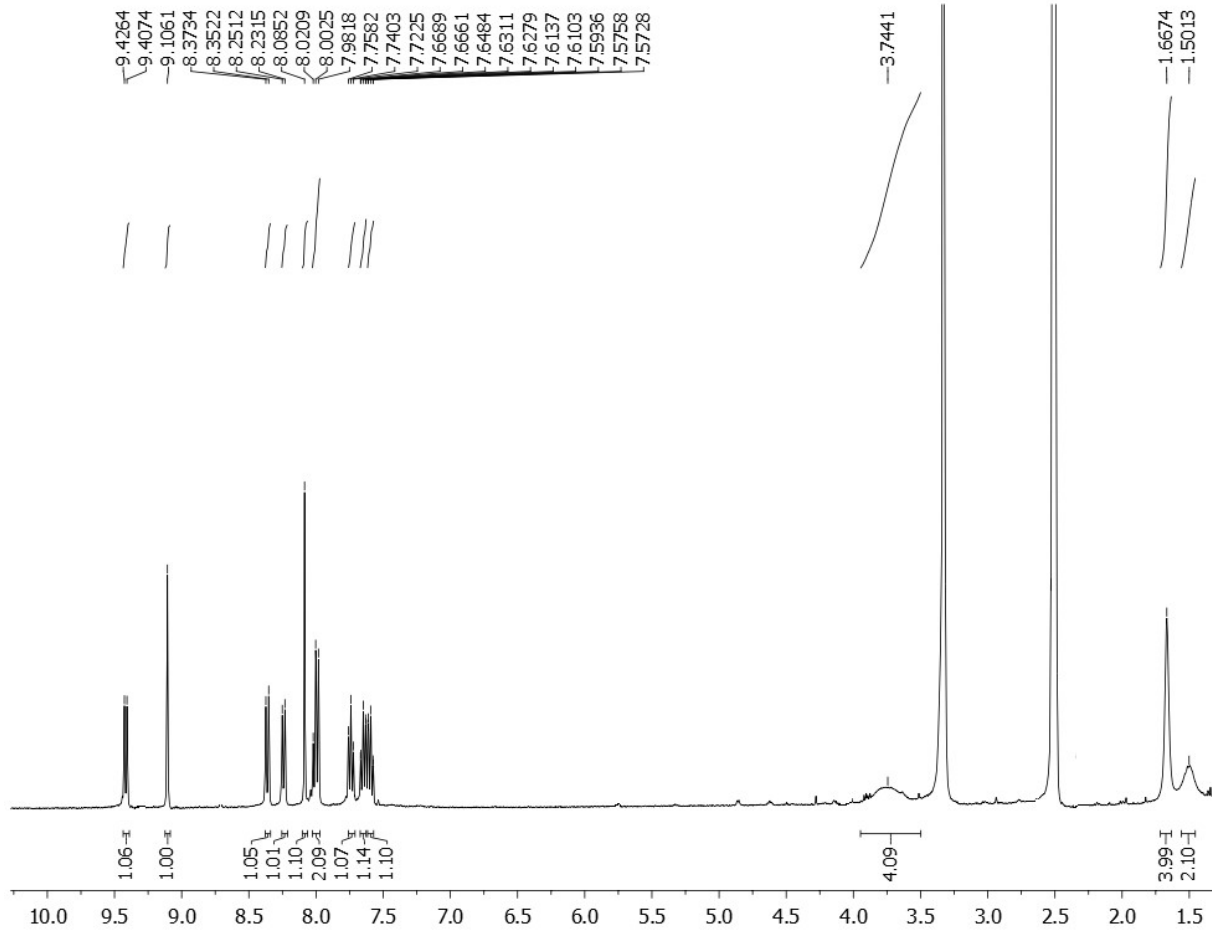


**Figure S54.**  $^1\text{H}$  NMR spectrum (DMSO- $d_6$ , 400 MHz) of *benzo[g]benzo[4,5]imidazo[1,2-a][1,8]naphthyridin-6-yl(piperidin-1-yl)methanone* **26**

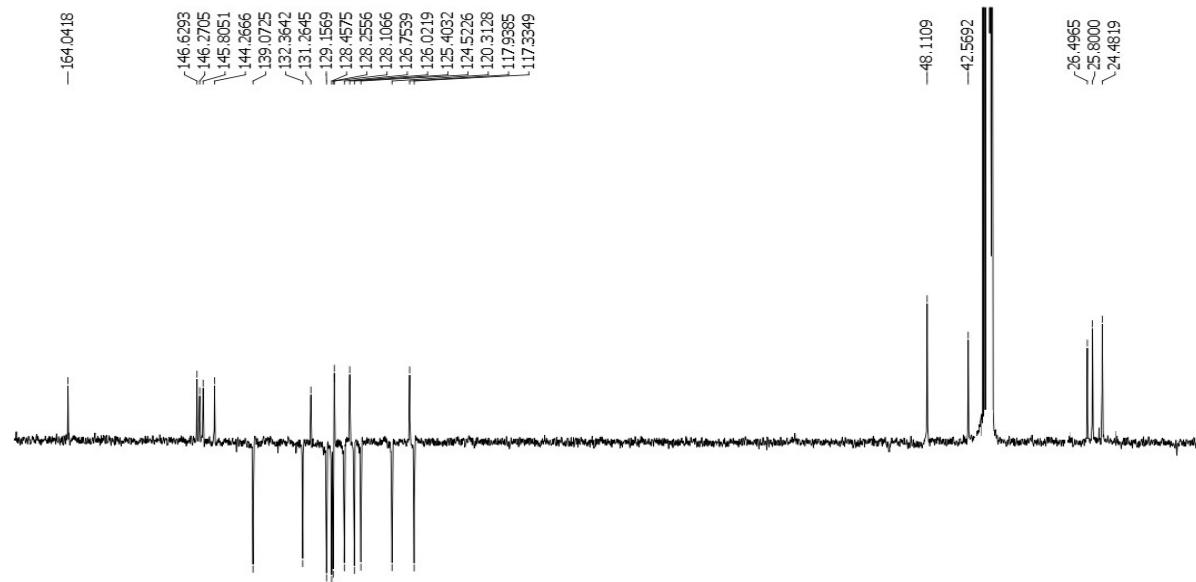


**Figure S55.**  $^{13}\text{C}$  NMR spectrum (DMSO- $d_6$ , 100 MHz) of *benzo[g]benzo[4,5]imidazo[1,2-a][1,8]naphthyridin-6-yl(piperidin-1-yl)methanone* **26**

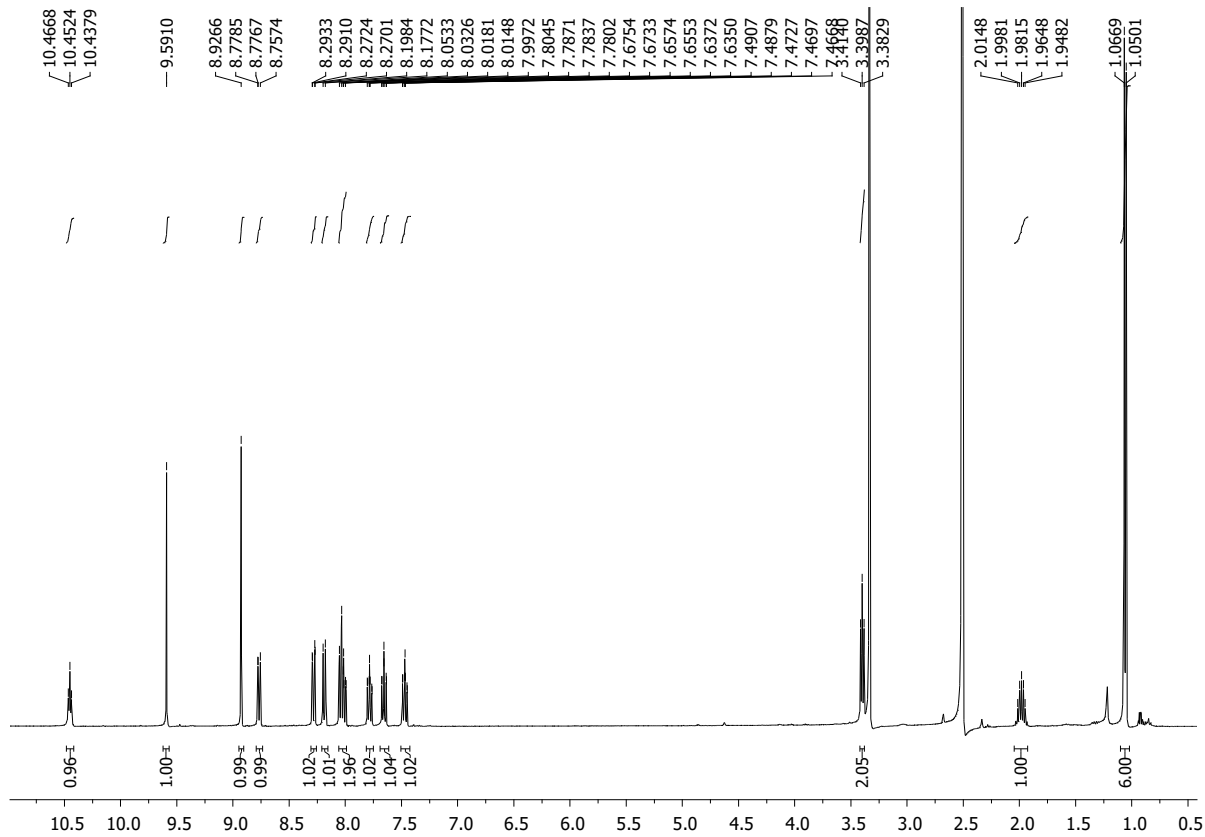


**Figure S56.**  $^1\text{H}$  NMR spectrum (DMSO- $d_6$ , 400 MHz) of *N*-isobutylbenzo[*g*]benzo[4,5]imidazo[1,2-*a*][1,5]naphthyridine-7-carboxamide **29**

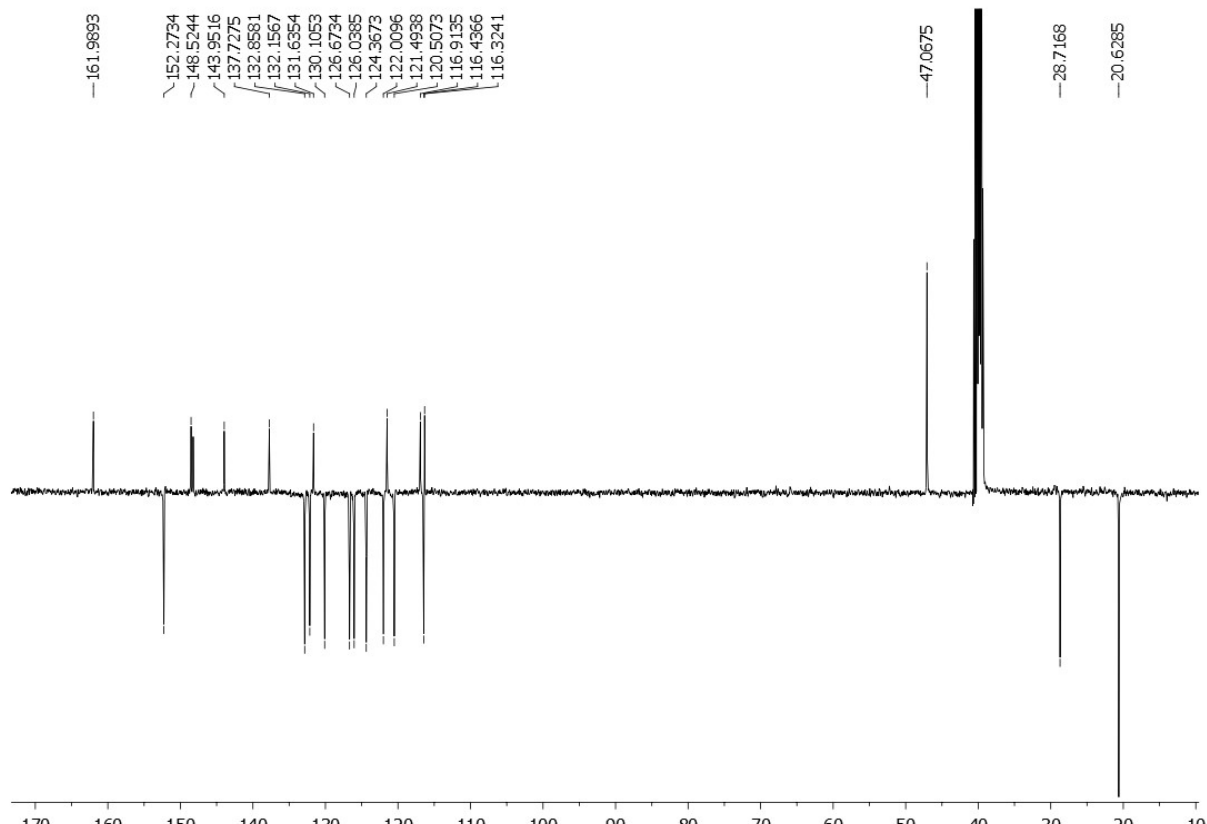


**Figure S57.**  $^{13}\text{C}$  NMR spectrum (DMSO- $d_6$ , 100 MHz) of *N*-isobutylbenzo[*g*]benzo[4,5]imidazo[1,2-*a*][1,5]naphthyridine-7-carboxamide **29**

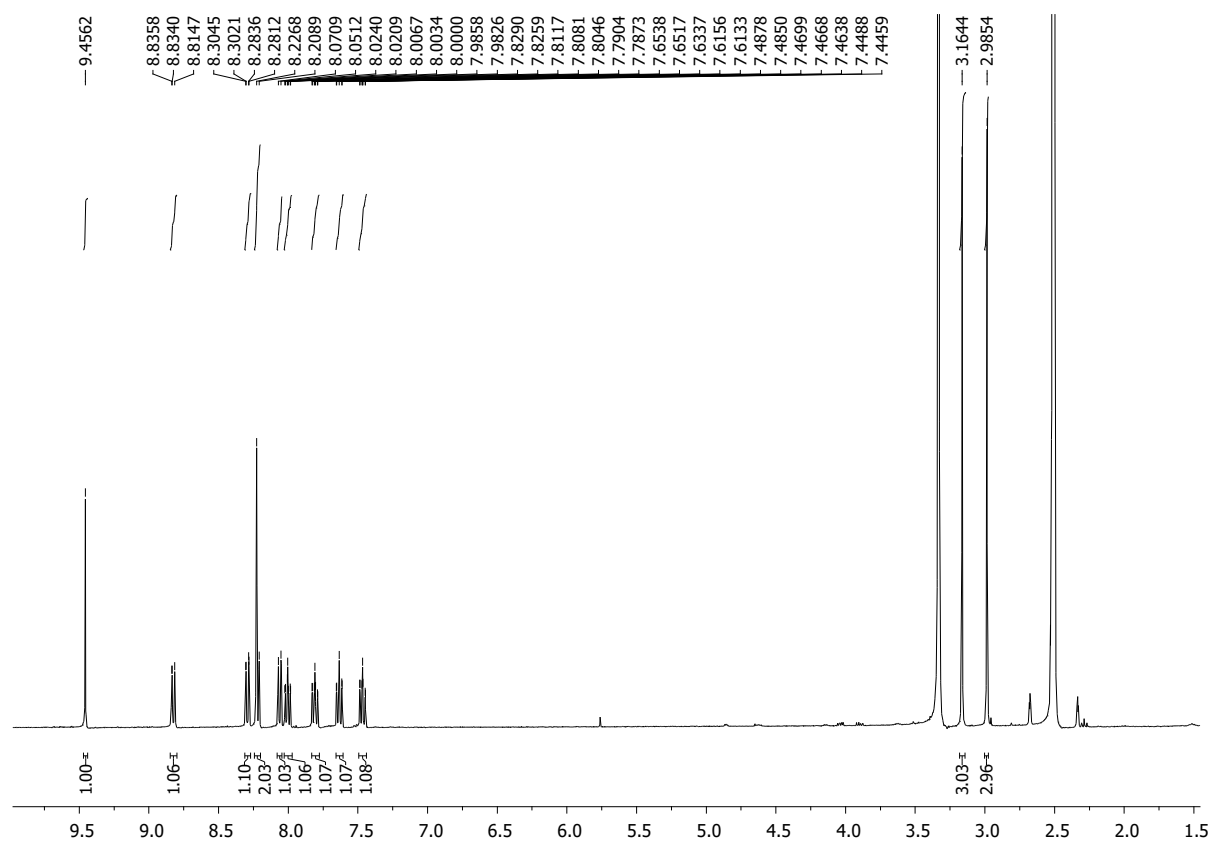


**Figure S58.**  $^1\text{H}$  NMR spectrum (DMSO- $d_6$ , 400 MHz) of *N,N*-dimethylbenzo[*g*]benzo[4,5]imidazo[1,2-*a*][1,5]naphthyridine-7-carboxamide **30**

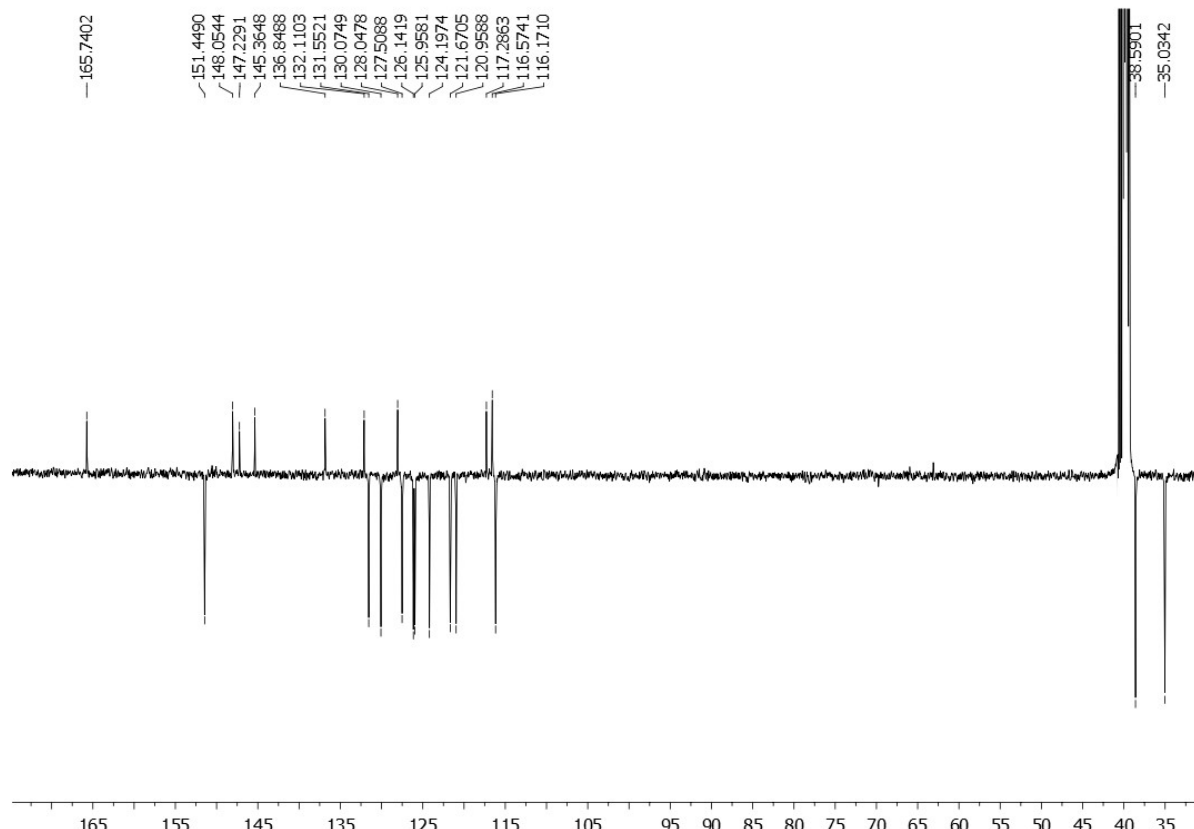


**Figure S59.**  $^{13}\text{C}$  NMR spectrum (DMSO- $d_6$ , 100 MHz) of *N,N*-dimethylbenzo[*g*]benzo[4,5]imidazo[1,2-*a*][1,5]naphthyridine-7-carboxamide **30**